Self-avoiding walks in Constrained and Random Geometries: Series Studies

Anthony J. Guttmann[a]

[a]Department of Mathematics and Statistics, The University of Melbourne,
Victoria, 3010, Australia
ARC Centre of Excellence for the Mathematics and Statistics of Complex Systems.

The self-avoiding walk is an excellent representation of an isolated polymer chain in dilute solution, as well as being a classical combinatorial problem. It lends itself to modelling many other situations by modifying the nature of monomer-monomer and other interactions. Randomness can be introduced either in the surrounding environment, or within the walk itself. In this chapter we discuss a variety of series studies of random self-avoiding walks, with both types of randomness, as well as series studies of self-avoiding walks in constrained geometries. In the latter case, one can consider interactions between the walk and the wall of the confining geometry, as well as inter-monomer interactions. A variety of interesting physical phenomena can be so modelled, and we discuss series studies of a variety of chemical and biological phenomena. These include the denaturation of DNA, the "pulling" of a macromolecule, such as DNA, away from an adsorbing surface, and the collapse transition of a vesicle.

1. INTRODUCTION

This topic is sufficiently large that an entire book could be devoted to it, and still not give complete coverage. Reviews by Barat and Chakrabati [1] on SAW on random lattices, and by Soteros and Whittington [2] on random copolymers are individually of comparable length to this chapter, yet discuss just two of several topics addressed here. Thus this chapter consists of a (hopefully representative) selection of topics that inevitably reflects both the expertise and personal taste of the author. Knowledge of the fundamentals of the theory of SAW, and of series generation and analysis are assumed. A good introduction to these can be found in [3], where the problem of SAW in a constrained geometry is also briefly discussed.

We will initially discuss SAW in random geometries, and then SAW in constrained environments. In the former case, many of the studies have used methods other than series analysis, typically Monte Carlo, and so our discussion of this topic will be briefer than that of SAW in constrained geometries.

For SAW in random geometries, the randomness can be in the environment, for example SAW on a regular lattice with randomly missing sites or bonds. We discuss this situation in the next section. Alternatively, the randomness can be in the walk itself, which is typically the case with copolymers, in which the SAW comprises more than one type of

monomer, each having different interaction properties, and with the monomers randomly distributed. We discuss this situation in section 3.

We subsequently consider the problem of SAW in restricted geometries, confined to a wedge, a strip, a slab, a square or a cube. We then discuss SAW on non-regular lattices, such as the Penrose and Ammann-Beenker tilings.

Finally, we discuss variants of the SAW designed to model a variety of biological phenomena, notably DNA denaturation, the collapse of a vesicle, and the pulling of a macromolecule from an adsorbing surface by an applied force normal to the surface.

While the primary focus of this chapter is on series methods, it has been necessary to make reference to other approximation techniques, such as Monte Carlo methods and renormalization group methods in order to assess the reliability of certain results. It has also been necessary to provide some background to a number of the problems discussed, as these are unlikely to be familiar to many readers. Finally, certain rigorous results have been discussed, as it is necessary to focus on what is rigorously known, what is exactly known (but not rigorously), and what is conjectural. To put these into focus, the *existence* of the connective constant, or growth constant, of a SAW is rigorously known. The value of the critical exponent $\nu = 3/4$ for SAW on a regular two-dimensional lattice is exactly known, where ν is the critical exponent characterising the growth of the mean square end-to-end distance of an n-step SAW. The corresponding quantity for three-dimensional SAW is known only numerically, and hence approximately.

We will first very briefly review the properties of SAW on a regular, hypercubic lattice $\mathbb{Z}^d$, in particular those on the square lattice $\mathbb{Z}^2$. For walks on an infinite lattice, it is generally accepted [4] that the number of such walks of length n, equivalent up to a translation, grow as $c_n \sim const.\mu^n n^{\gamma-1}$, with metric properties, such as mean-square radius of gyration or mean-square end-to-end distance growing as $\langle R^2 \rangle_n \sim const.n^{2\nu}$, where $\gamma = 43/32$ and $\nu = 3/4$. The growth constant μ is lattice dependent, and for the honeycomb lattice is believed to be $\mu_{honey} = \sqrt{(2+\sqrt{2})}$ [5], while for the square lattice it is not known exactly, but is indistinguishable numerically from the unique positive root of the equation $13x^4 - 7x^2 - 581 = 0$ [6]. In three dimensions the growth constants and exponents are known only approximately, and are not believed to be algebraic (the growth constants) or rational (the exponents).

We denote the SAW generating function by $C(x) := \sum_n c_n x^n$, and it will be useful to define a second generating function for those SAW which start at the origin $(0,0)$ and end at a given point (u,v), as $G(0,0;u,v)$. In terms of this generating function, the mass m is defined [4] to be the rate of decay of G along a coordinate axis,

$$m := \lim_{n\to\infty} \frac{-\log G(0,0;n,0)}{n}. \tag{1}$$

where we have assumed isotropy, so that the choice of co-ordinate direction is irrelevant.

2. SELF-AVOIDING WALKS IN RANDOM GEOMETRIES

Consider a SAW on a lattice in which some sites are missing. One can remove sites at random, such that a fraction p of sites is removed, and study the behaviour of SAW averaged over an ensemble of such lattices. Thus one obtains the properties of the SAW

averaged over a uniform distribution of such lattices. This is the *quenched* situation. Brief reflection allows one to conjecture the effect of this site dilution. Firstly, it is clear that the problem now becomes one of SAW on a percolation cluster. For $p > p_c$ there is no infinite cluster, and hence all SAW are of finite length. For $p < p_c$, the average number of neighbours of a lattice site is modified from q, the coordination number of the undiluted lattice, to $q(1-p)$. Thus one would expect the growth constant μ also to be reduced, and $\mu(p)$ to be a monotone decreasing function of p for $0 < p < p_c$. What is less clear is how the critical exponents behave. As discussed above, for the undiluted lattice one has $\langle R^2 \rangle_n \sim const.n^{2\nu}$ in the limit as n becomes large. The exponent ν is given phenomenologically by the Flory formula, $\nu = 3/(d+2)$ which seems to be exact for $d = 2$ and $d = d_c = 4$ (ignoring logarithmic corrections at $d = d_c = 4$). The Flory formula prediction is about 2% high at $d = 3$. Above four dimensions the exponent "sticks" at the value $1/2$, as the SAW constraint becomes increasingly irrelevant. Field theory, again for the undiluted lattice [7], gives $\nu = 1/2 + \epsilon/16 + 15\epsilon^2/512 + \ldots$, where $\epsilon = 4 - d$.

Naive application of the Harris criterion [8] would suggest that for $p_c > p > 0$ the exponents would be modified. That is to say, the slightest level of disorder would be sufficient to change the exponent. Loosely speaking, the Harris criterion says that the universality class of a system is affected by the presence of disorder if the specific heat exponent α of the pure system is positive. For both two- and three-dimensional SAW this is the case. For $d = 2$, $\alpha = 1/2$, while for $d = 3$, $\alpha \approx 0.236$. However, as SAW are given by the $N \to 0$ limit of the O(N) model, a modified Harris criterion applies [8]. In the usual Harris criterion argument, one can relate the concentration induced change in transition temperature to the correlation length, and then using the hyperscaling relation $d\nu = 2 - \alpha$ deduce that if $\alpha > 0$, the exponent ν will change with impurity concentration $p > 0$, no matter how small. However, in the $N \to 0$ limit, the transition temperature change *does not* depend on α, but only on the dimensionality of the system. Thus weak disorder is not expected to modify the universality class.

However, at $p = p_c$ we are in a regime of strong disorder, and one expects a change in universality class. This situation was first discussed within the framework of the epsilon expansion by Meir and Harris [9] in 1989, and demonstrated numerically by Grassberger [10] in 1993. The epsilon expansion has recently been extended by von Ferber et al. [11], who found that at $p = p_c$ one has $\nu_c = 1/2 + \epsilon/42 + 110\epsilon^2/21^3 + \ldots$ where now $\epsilon = 6 - d$. The appropriate Flory formula [12] is now $\nu_c = 3/(d_p+2)$, where $d_p = d - \beta_p/\nu_p$ and β_p and ν_p are the appropriate percolation exponents. In two dimensions we have $\beta_p = 5/36$ and $\nu_p = 4/3$, hence $d_p = 91/48$ and $\nu_c = 144/187 = 0.7700\ldots$. In [9] the values 0.76 ± 0.08, 0.67 ± 0.04, 0.63 ± 0.02 and 0.54 ± 0.02 were obtained for $d = 2, 3, 4, 5$ respectively, based on the analysis of short series. Grassberger [10] obtained $v = 0.783 \pm 0.003$ by Monte Carlo analysis, while Lam [13] estimated $\nu_c = 0.81 \pm 0.03$. The most recent series work, [14] finds $\nu_c = 0.778 \pm 0.015$ and $\nu_c = 0.787 \pm 0.010$ from two different analyses of the two-dimensional case, and $\nu_c = 0.662 \pm 0.006$ in the three-dimensional case. These are consistent with recent Monte Carlo analyses, and also with the epsilon-expansion given above, which evaluates to $\nu_c = 0.785....$ and $\nu_c = 0.678...$ for two- and three-dimensions respectively. Thus all numerical work and theory is in reasonable agreement, and this situation can be considered to be well understood.

3. RANDOM COPOLYMERS

For the problem of random copolymers, unlike the situation discussed in the previous section, the randomness is now *not* in the medium, but in the SAW itself. One of the simpler cases is when there are two types of monomer, say A and B. Typically one has a fraction p of A-type monomers, and a fraction $(1-p)$ of B-type monomers. One usually assumes that the monomers are randomly distributed and constrained only by the value of p. An excellent contemporary review of this topic can be found in [2]. More generally, one can consider the case with k types of monomer, denoted $m_1, \ldots, m_k$, where the state of the polymer, modelled by an n-step SAW, is given by an n-tuple $\alpha = \alpha_1, \ldots, \alpha_n$, where $\alpha_i \in \{m_1, \ldots, m_k\}$. The values of α_i are taken from some distribution, appropriately chosen to model the problem at hand. In [2] three representative situations are discussed. The first is adsorption of a copolymer onto a surface, the second is the localization of a copolymer at an interface between two immiscible liquids, and the third is the temperature- or solvent-induced coil-ball collapse of a copolymer. We discuss these three representative problems below.

We will consider the case of an isolated SAW, of length n. Two types of averaging are usually considered, corresponding to the *quenched* and *annealed* cases respectively. In the quenched case, the average is taken of the logarithm of the partition function over the entire distribution, so that the free energy is

$$\mathcal{F}_q := \lim_{n\to\infty} \frac{1}{n} \langle \log Z_n \rangle, \tag{2}$$

while in the annealed case

$$\mathcal{F}_a := \lim_{n\to\infty} \frac{1}{n} \log \langle Z_n \rangle. \tag{3}$$

The averages are taken over all α. It is noteworthy that the annealed free energy is an upper bound on the quenched free energy. This is useful as the former is usually easier to calculate. Better approximations are often provided by the Morita [15] approximation and the replica method. We refer readers to [2] and references therein for further details.

We will now consider the three problems referred to above. Random copolymer adsorption refers to the situation in which a copolymer (most simply described as one with two types of monomer, say A and B) is adsorbed onto a surface. Consider an n-step SAW, with a proportion p of A type monomers, and a proportion $1-p$ of B type monomers in a half-space. In two dimensions we are therefore referring to that section of $\mathbb{Z}^2$ with $y \geq 0$. Let the origin of the SAW lie in the line $y = 0$. Finally, the energy comes from the A monomers in the line $y = 0$. That is to say, only the A monomers are attracted to the surface. There is no surface interaction with B monomers. For those SAW, with cardinality $c_n^+(v_A|\alpha)$ with v_A vertices in $y = 0$, and monomer distribution as described above given by α, where $\alpha_i = 1$ if the i^{th} vertex is A and zero otherwise, the partition function is given by

$$Z_n^+(\kappa|\alpha) = \sum_{v_A} c_n^+(v_A|\alpha) \exp(\kappa v_A). \tag{4}$$

For technical reasons one usually insists that the last step of the SAW also lies in the line $y = 0$, so that we are studying self-avoiding loops, rather than SAW. The reason for this

restriction is that it allows concatenation of such walks, and hence application of standard tools like sub-additivity, which are so ubiquitous in existence proofs of free-energies and the like.

What makes this problem so difficult—and indeed most copolymer problems difficult—is the necessity to take the average over all possible 2^n distributions of monomers on the polymer. Nevertheless, some exact enumeration studies of this problem have been conducted. Martin [16] estimated the location of the transition using exact enumeration methods. An open question is the value of the crossover exponent, ϕ, which describes the shape of the free-energy near the adsorption critical temperature. The conclusion from the above study, and others, is that the difference between this exponent and its homopolymer counterpart, if it exists, is too small to be detectable by any current numerical studies.

The second problem of considerable interest is that of localization of a copolymer. Consider a mixture of two immiscible liquids such as oil and water. Then consider a copolymer, modelled as usual by a SAW, with two kinds of monomer, distributed uniformly and independently, and with origin at the interface between the two liquids. Let A monomers be energetically attracted to the water phase and B monomers to the oil phase. At high temperatures, the SAW will sit entirely in the liquid that gives rise to the lowest energy configuration. At low temperatures however, the SAW will try to orient itself with A monomers in the water and B monomers in oil. It will thus cross the interface frequently. This is the so called *localized* phase, as in it the SAW is largely constrained to the vicinity of the interface. As the temperature is raised, one expects a phase transition to a delocalized phase, heralded by a singularity in the quenched free energy. The model can also be generalized to include an interaction energy for monomers in the interface.

James et al. [17] and Martin et al. [18] studied the localization problem for the simple-cubic lattice $\mathbb{Z}^3$, where the plane $z = 0$ defines the interface. Most of their studies are devoted to establishing rigorous results, of the existence and convexity type, and determining qualitatively the shape of the phase diagram.

The third problem we will consider is the collapse of copolymers. In the homopolymer case (where there is only one type of monomer), the collapse transition is known to take place at the θ temperature, brought about by sufficiently strong attractive interactions between nearest neighbour monomers that are not joined by a path of the SAW. In that case, the exponent ν that characterises metric properties such as the mean-square end-to-end distance and the radius of gyration, which are characterised by the exponent ν, changes abruptly to ν_θ at the θ temperature, and then to $\nu_c = 1/d$ at lower temperatures, when the SAW collapses into a d-dimensional ball.

In the copolymer case, the simplest realistic model is as usual to have A monomers with probability p and B monomers with probability $1 - p$. Then instead of just considering interactions between nearest neighbour contacts, as in the homopolymer case, we associate different energies to AA, BB and AB contacts. Typically, one allows like monomers to attract and unlike monomers to repel, or vice versa. In the former case we have a model of hydrophilic and hydrophobic monomers, and in the latter case we have a model of a highly screened Coulomb system.

Golding and Kantor [19] and Kantor and Kardar [20] studied a version of this problem by both exact enumeration and Monte Carlo methods. In the former situation described above, they find a collapse transition much like the transition discussed above in the

homopolymer case, which holds irrespective of the ratio of type A to type B monomers. In the latter situation, modelling a screened Coulomb system, the behaviour depends on the ratio of the two types of monomers. If this is around 1, so that the two types of monomer have similar cardinality, the system has no nett charge, and there is a collapse transition. But if the monomer ratio is substantially different from 1, the repulsive interactions between the monomers that are in excess prevent any collapse, and the SAW remains in its coiled state at all temperatures. A later enumeration study by Monari and Stella [21] considered the system with equal numbers of A and B monomers and a Coulombic interaction energy. They found that at the θ temperature, the radius of gyration exponent ν and the crossover exponent ϕ were indistinguishable from their homopolymer values in both two- and three-dimensions.

Many features of this fascinating problem have not been mentioned here, but can be found in the comprehensive and up-to-date review of random copolymers in [2]. In particular, many of the rigorous results and the numerical results obtained both by other approximation methods and by Monte Carlo methods which have not been discussed here can be found there

4. SAW IN WEDGES

In this section we consider the effect of confining a SAW to a *wedge*, formed by the intersection of two (non-parallel) $d-1$-dimensional planar surfaces in a d-dimensional hypercubic lattice, with co-ordinates labelled by $\{x_\delta | \delta = 1, 2, \ldots, d\}$. The surfaces intersect in a $d-2$ dimensional surface perpendicular to both x_1 and x_2, with wedge angle α.

It is not difficult to show that the growth constant μ remains unchanged for most "obvious" geometries, such as the semi-infinite lattice, or indeed any positive wedge angle. A much more subtle result was proved by Hammersley and Whittington [22] who considered SAW confined to a subset $\mathbb{Z}^d(f)$ of the d-dimensional hypercubic lattice, such that the co-ordinates $(x_1, x_2, \ldots, x_d)$ of each walk vertex satisfy $x_i \geq 0$ and $0 \leq x_k \leq f_k(x_1)$ for $k = 2, 3, \ldots, d$. They showed that the growth constant remains unchanged provided that $f_k(x) \to \infty$ as $x \to \infty$.

In this problem, either end of a walk can be in the bulk, at a surface, or at the wedge "edge". This gives rise to a number of possible generating functions, and we now develop the theory in terms of the general N-vector model, and take the limit $N \to 0$ in order to recover the SAW situation. Expressed as a problem in the framework of the O(N) model, the Hamiltonian is

$$\mathcal{H} = -K \sum_{<i,j>} \sigma_i \cdot \sigma_j - L_0 \sum_i \sigma_i^{(1)} - L_1 \sum_i{}' \sigma_i^{(1)} - L_2 \sum_i{}'' \sigma_i^{(1)} \tag{5}$$

where σ_i is an N-dimensional unit vector with components $(\sigma_i^{(\beta)}, \beta = 1, 2, \ldots, N)$ and L_0, L_1 and L_2 are bulk, surface and edge fields respectively, all parallel to $\sigma_i^{(1)}$. The first sum is over nearest-neighbour pairs, the second is over all spins, the third is over all spins in a surface, and the fourth is over all edge spins. The edge magnetization is the expectation value of an edge spin:

$$m_2(K; L_0, L_1, L_2) = \langle \sigma_i^{(1)}(x_1 = 0 = x_2) \rangle. \tag{6}$$

Differentiation with respect to the three fields L_0, L_1 and L_2 allows for three susceptibilities to be naturally defined, viz:

$$\chi_2 \sim const.t^{-\gamma_2}, \tag{7}$$

$$\chi_{21} \sim const.t^{-\gamma_{21}}, \tag{8}$$

$$\chi_{22} \sim const.t^{-\gamma_{22}}, \tag{9}$$

where $t = T/T_c - 1$. If we now write the free energy in the form

$$\mathcal{F} = V f_b + A f_s + L f_e + \ldots \tag{10}$$

where V is the 'volume' of the system, A is the 'area' of the surface, and L is the 'length' of the edge, then f_b, f_s and f_e denote the bulk, surface and edge free energies respectively.

Standard scaling theory informs us that in this case, with three fields, the singular part of the free-energy will scale as:

$$f_{sing} = \lambda^{-d} f(\lambda^{y_0} g_0, \lambda^{y_1} g_1, \lambda^{y_2} g_2) \tag{11}$$

where y_0, y_1 and y_2 are the renormalization group eigenvalues associated with the three fields. The three free energies referred to above can be written in terms of the canonical scaling form as

$$f_b \sim t^{2-\alpha} \Psi_b(h t^{-y_0 \nu}), \tag{12}$$

$$f_s \sim t^{2-\alpha_s} \Psi_b(h t^{-y_0 \nu}, h_1 t^{-y_1 \nu}), \tag{13}$$

$$f_e \sim t^{2-\alpha_e} \Psi_b(h t^{-y_0 \nu}, h_1 t^{-y_1 \nu}, h_2 t^{-y_2 \nu}), \tag{14}$$

where y_0, y_1 and y_2 are the bulk, surface and edge scaling indices, and

$$(2-\alpha) = d\nu, \ (2-\alpha_s) = (d-1)\nu, \text{ and } (2-\alpha_e) = (d-2)\nu. \tag{15}$$

All susceptibilities now follow by taking the appropriate derivatives, so that

$$\chi = \frac{\partial^2 f_b}{\partial h^2} \sim const.t^{-\gamma}, \tag{16}$$

$$\chi_1 = \frac{\partial^2 f_s}{\partial h \partial h_1} \sim const.t^{-\gamma_1}, \tag{17}$$

$$\chi_{11} = \frac{\partial^2 f_s}{\partial h_1^2} \sim const.t^{-\gamma_{11}}, \tag{18}$$

$$\chi_2 = \frac{\partial^2 f_e}{\partial h \partial h_2} \sim const.t^{-\gamma_2}, \tag{19}$$

$$\chi_{21} = \frac{\partial^2 f_e}{\partial h_1 \partial h_2} \sim const.t^{-\gamma_{21}}, \tag{20}$$

$$\chi_{22} = \frac{\partial^2 f_e}{\partial h_2^2} \sim const.t^{-\gamma_{22}}, \tag{21}$$

and by performing these differentiations, we immediately find

$$\gamma = \nu(2y_0 - d) \tag{22}$$

$$\gamma_1 = \nu(y_0 + y_1 - d + 1) \tag{23}$$

$$\gamma_{11} = \nu(2y_1 - d + 1) \tag{24}$$

$$\gamma_2 = \nu(y_0 + y_2 - d + 2) \tag{25}$$

$$\gamma_{21} = \nu(y_1 + y_2 - d + 2) \tag{26}$$

$$\gamma_{22} = \nu(2y_2 - d + 2). \tag{27}$$

These results can be combined to produce the scaling law

$$2\gamma_1 - \gamma_{11} = \gamma + \nu, \tag{28}$$

which was first derived by Barber [23], and the additional scaling laws,

$$2\gamma_2 - \gamma_{22} = \gamma + 2\nu, \tag{29}$$

and

$$2\gamma_{21} - \gamma_{22} = \gamma_{11} + \nu, \tag{30}$$

first given by Guttmann and Torrie [24].

The susceptibilities can also be defined in terms of correlation functions, which will be useful in taking the $N \to 0$ limit of the O(N) model. Define the correlation function

$$C(\mathbf{r}' = \mathbf{0}; \rho, x_1, x_2) \tag{31}$$

between a spin at the edge ($\mathbf{r}' = \mathbf{0}$) and a spin at (ρ, x_1, x_2) where ρ is a $(d-2)$-dimensional vector with components $x_3, x_4, \ldots, x_d$. First, note that the correlation function will depend on the orientation of the vector (ρ, x_1, x_2) even near T_c. Denote its magnitude by r, its orientation within the (x_1, x_2) plane by θ (clearly $0 \le \theta \le \alpha$), where α is the wedge angle, and its orientation within the surface plane by ϕ.

For $T > T_c$ we have

$$C(r, \theta, \phi) \sim_{r\to\infty} f(r, \theta, \phi) \exp[-r/\xi_{\theta,\phi}(t)], \tag{32}$$

where f decays more slowly than the exponential term. At $T = T_c$,

$$C(r, \theta, \phi) \sim_{r\to\infty} A(\theta, \phi)/r^{d-2-\eta_{\theta,\phi}}, \tag{33}$$

which leads to the special cases $\eta_2 = \eta$ for $(\theta > 0, \phi > 0)$, $\eta_{2,1}$ for $(\theta = 0, \phi > 0)$, and $\eta_{2,2}$ for $(\theta = 0, \phi = 0)$. Clearly $\eta_2 \le \eta_{21} \le \eta_{22}$ as there are more possible paths leading to η_2 than the others, and similarly for the last inequality.

A typical susceptibility is

$$\chi_2 = \sum_{\rho} \sum_{x_1=0}^{\infty}{}' \sum_{x_2=0}^{\infty} C(\mathbf{r}' = \mathbf{0}; \rho, x_1, x_2) \tag{34}$$

with a similar expression holding for the other susceptibilities. (The prime is to remind one of the restriction $\pi \leq \alpha$). Following an argument of Sarma, given in the appendix to a paper by Daoud et al. [25], we see that χ_2 is the generating function for SAW in the wedge, with one end tethered to the edge, and no restrictions on the other end. χ_{21} is given by the generating function for SAW with one edge tethered to the edge, and the other end in the surface, while χ_{22} is given by the generating function for SAW with both edges tethered to the edge. Replacing sums by integrals in the above expression, it is straightforward to show that

$$\gamma_2 = \nu(2 - \eta_2), \tag{35}$$

$$\gamma_{12} = \nu(1 - \eta_{12}), \tag{36}$$

$$\gamma_{22} = -\nu\eta_{22}. \tag{37}$$

Defining $\eta_{00} = \eta$, and $\eta_{i0} = \eta_i$ these expressions can be combined to give

$$\eta_{pq} = (\eta_{pp} + \eta_{qq})/2,$$

a result first obtained by Cardy [26] from field-theoretical arguments.

Based on extensive enumerations in wedges of various angles, Guttmann and Torrie [24] found compelling numerical evidence for SAW in two-dimensional wedges of angle α, that $y_2 = -5\pi/8\alpha$. If one recalls that $y_0 = 91/48$ and $y_1 = 3/8$ were already known, it follows that all exponents for the edge problem follow. Cardy subsequently verified this conjecture for $y_2(\alpha)$, again from field theoretical arguments. For three-dimensional SAW, the enumerations in [24] led to the conjecture $y_2(\alpha) = 1/2 - 0.85(2)/\alpha$. Both these results can be compared to the mean-field theory result, $y_2^{MF} = 1 - d/2 - \pi/\alpha$. Note that the mean-field result agrees with the enumeration results in both the constant term and the form of the angular dependence.

An interesting and physically significant generalisation of this problem can be achieved by associating a fugacity with those monomers lying in the surface, or surfaces, in the case of a wedge geometry. If the fugacity is sufficiently attractive then at some critical temperature the SAW becomes adsorbed onto the surface. In an interesting paper, Hammersley, Torrie and Whittington [27] considered the simpler case of a single surface (corresponding to $\alpha = \pi$) on the hypercubic lattice and showed that there must be a phase transition. In [28], Batchelor et al. studied the problem of two-dimensional SAW, and more general SAW networks in which the surface is allowed to assume a variety of boundary conditions on either side of the wedge. That is to say, there is a different fugacity associated with SAW contacts in one surface to that in the other surface. As a result of this study, they were able to give conjectured exponents for an arbitrary polymer network—that is to say, not just SAW, but stars—connected to the surface of an arbitrary wedge (in two dimensions) where the surface is allowed to have general mixed boundary conditions.

5. SELF-AVOIDING WALKS IN STRIPS AND SLABS

Consider SAW in a strip of width L on the square lattice. This is essentially a one-dimensional problem. Indeed, the column-to-column transfer matrix is finite, and hence by a well-known theorem [29] the generating function is rational. The "critical exponent"

is 1, corresponding to a simple pole, and the number of SAW of length n, which we denote $c_n(L) \sim const.\mu(L)^n$, where the growth constant (sometimes called the *connective constant*, though this latter term is also applied to the logarithm of μ by some authors) is a strictly monotone increasing function of L [22], and $\lim_{n\to\infty} \mu(L) = \mu$, the growth constant in the (two-dimensional) bulk case. The generating functions have been investigated for small values of L in [30]. Daoud and de Gennes [31] has given a scaling argument for the L dependence of $\mu(L)$, which leads to $\log\mu - \log\mu(L) \sim D_w L^{-1/\nu}$, where $\nu = 3/4$ as usual denotes the exponent that characterises the mean-square end-to-end distance of an n-step SAW, and D_w is an amplitude.

An interesting point occurs if we consider self-avoiding polygons, similarly constrained. An n-step self-avoiding polygon (SAP) is a subset of $(n-1)$-step SAW; those with adjacent end-points. Clearly, joining the end-points results in an n-step SAP. By identical arguments we see that the generating function of SAP in a strip is rational. The "critical exponent" is 1, corresponding to a simple pole, and the number of SAP of perimeter n, which we denote $p_n(L) \sim const.\mu_p(L)^n$, where the growth constant is a monotone increasing function of L, and $\lim_{L\to\infty} \mu_p(L) = \mu$. However, [32] $\mu_p(L) < \mu(L)$, even though these two quantities have the same limit as L becomes infinite. This follows from Kesten's pattern theorem [32], which, crudely speaking, says that if a SAW pattern in one geometry can occur at least three times, and it cannot occur in a different geometry, then SAW in the former class are exponentially more numerous than those in the latter. Soteros and Whittington [32] displayed such a pattern for SAW in strips of finite widths, hence the above result follows. As a similar scaling Ansatz applies for SAP, viz: $\log\mu - \log\mu(L) \sim D_p L^{-1/\nu}$, it follows that $D_w \neq D_p$.

We can make use of existing results in the literature to quantify this effect. In [30] the growth constants for SAW and SAP in a strip of width L are given, for $L \leq 6$. Using these results, and Daoud and de Gennes's scaling form above, we find $D_w/D_p \approx 0.52$.

For a slab geometry, corresponding to SAW constrained between two parallel planes, which is essentially a two-dimensional problem, there is no similar pattern, and one has the same growth constant for SAW and SAP confined between two planes separated by a distance L [33]. The reason for this difference is, loosely speaking, that it is easy to devise "blocking" patterns for SAW in strips, but not in slabs, where the extra dimension allows the SAW to avoid the blockage. The generating function is no longer rational in this geometry, but the strictly monotone increasing property of the growth constant with separation L still prevails [22].

6. SELF-AVOIDING WALKS IN SQUARES AND CUBES

Another interesting constrained SAW problem is that of SAW confined to lie entirely within a square, or rectangle. We will considering in detail the problem of self-avoiding walks on a subset of the square lattice $\mathbb{Z}^2$, though several of the theorems we give apply to the hypercubic lattice, and so hold for $\mathbb{Z}^d$, $d \geq 2$.

We are interested in a restricted class of square lattice SAW which start at the origin $(0,0)$, end at (L,L), and are entirely contained in the square $[0,L] \times [0,L]$. A fugacity x is associated with each step of the walk. Historically, this problem seems to have led two largely independent lives. One as a problem in combinatorics (in which case the fugacity

has been implicitly set to $x = 1$), and one in the statistical mechanics literature where the behaviour as a function of fugacity x has been of considerable interest, as there is a fugacity dependent phase transition.

The problem seems to have first been discussed by Abbott and Hanson [34] in 1978, many of whose results and methods are still the most powerful today. A key question considered both then and now, is the number of distinct SAW on the constrained lattice, and their growth as a function of the size of the lattice. Let $c_n(L)$ denote the number of n-step SAW which start at the origin $(0,0)$, end at (L,L) and are entirely contained in the square $[0,L] \times [0,L]$. Further, let $C_L(x) := \sum_n c_n(L)x^n$. Then $C_L(1)$ is the number of distinct walks from the origin to the diagonally opposite corner of an $L \times L$ lattice. In [34], and independently in [35] it was proved that $C_L(1) \sim const.\lambda^{L^2}$. The value of λ is not known, though bounds and estimates have been given in [34–36].

In the statistical mechanics literature, the problem appears to have been introduced by Whittington and Guttmann [35] in 1990, who were particularly interested in the phase transition that takes place as one varies the fugacity associated with the walk length. At a critical value, x_c the average walk length of a path on an $L \times L$ lattice changes from growing as L to growing as L^2. In [35] the critical fugacity was proved to be $\geq 1/\mu$, and conjectured to be $x_c = 1/\mu$, and in [37] the conjecture was proved.

In [34] the more general problem of SAW constrained to an $L \times M$ lattice was considered, where the analogous question was asked: how many non-self-intersecting paths are there from $(0,0)$ to (L,M). If one denotes the number of such paths by $C_{L,M}$, it is clear that, for M finite, the paths can be generated by a finite dimensional transfer matrix, and hence that the generating function is rational. Indeed, in [34] it was proved that

$$G_2(x) = \sum_{L \geq 0} C_{L,2}x^L = \frac{1-x^2}{1-4x+3x^2-2x^3-x^4}, \tag{38}$$

(where here we have corrected a typographical error). It follows that $C_{L,2} \sim \text{const.}\lambda_2^{2L}$, where $\lambda_2 = \sqrt{\frac{2}{\sqrt{13}-3}} = 1.81735\ldots$.

In [36] two further problems which can be seen as generalisations of the stated problem were considered. Firstly, they considered the problem in which SAWs are allowed to start anywhere on the left edge of the square and terminate anywhere on the right edge; so these are walks *spanning* the rectangle from left to right. Secondly, they considered the problem in which there may be several independent SAW, each SAW starting and ending on the perimeter of the square. The SAW are not allowed to take steps along the edges of the perimeter. Such walks partition the rectangle into distinct regions and by colouring the regions alternately black and white one gets a *cow-patch* pattern. Each problem is illustrated in fig. 1.

Following the work in [35], Madras in [37] proved a number of theorems. In fact, most of Madras's results were proved for the more general d-dimensional hypercubic lattice, but here we will quote them in the more restricted two-dimensional setting.

Let

$$\lambda_1(x) := \lim_{L \to \infty} C_L(x)^{1/L} \tag{39}$$

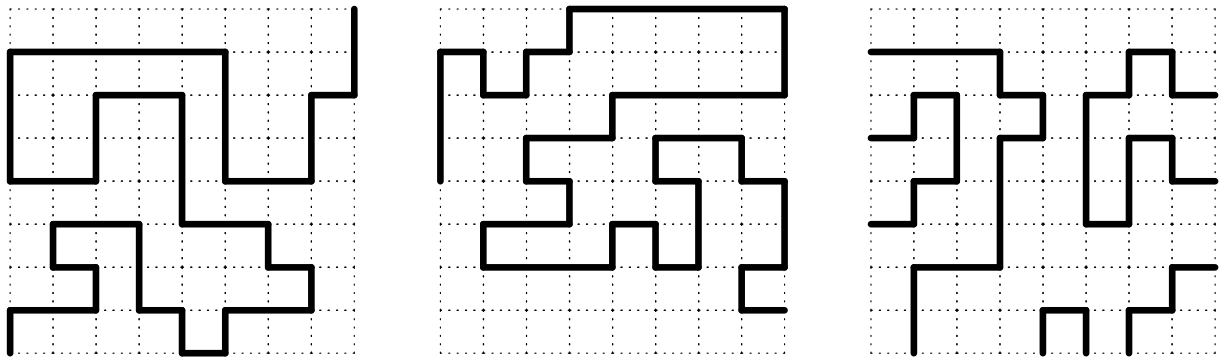

Figure 1. An example of a SAW configuration crossing a square (left panel), spanning a square from left to right (middle panel) and a cow-patch (right panel).

$$\lambda_2(x) := \lim_{L\to\infty} C_L(x)^{1/L^2} \tag{40}$$

Theorem 1. *(i) The limit (39) exists and is finite for* $0 \le x \le 1/\mu$*, and is infinite for* $x > 1/\mu$*. We have* $0 < \lambda_1(x) < 1$ *for* $0 < x < 1/\mu$ *and* $\lambda_1(1/mu) = 1$*.*
(ii) The limit (40) exists and is finite for all $x > 0$*. We have* $\lambda_2(x) = 1$ *for* $0 < x < 1/\mu$ *and* $\lambda_2(x) > 1$ *for* $x > 1/\mu$*.*

The average length of a walk is defined to be

$$\langle n(x)\rangle_L := \sum_n n c_n(L) x^n / \sum_n c_n(L) x^n. \tag{41}$$

In the next theorem, we use the notation $a \approx b$ to mean that there exist two positive constants C_1 and C_2 such that $C_1 b \le a \le C_2 b$.

Theorem 2. *As* $L \to \infty$*, we have* $\langle n(x)\rangle_L \approx L$ *for* $0 < x < 1/\mu$ *and* $\langle n(x)\rangle_L \approx L^2$ *for* $x > 1/\mu$*.*

The situation at $x = 1/\mu$ is unknown. Compelling numerical evidence is given in [36] that in fact $\langle n(1/\mu)\rangle_L$ is proportional to $L^{1/\nu}$, in accordance with an intuitive suggestion in [37].

Theorem 3. *For* $x > 0$*, define* $f_1(x) = \log \lambda_1(x)$ *and* $f_2(x) = \log \lambda_2(x)$*.*
(i) The function f_1 *is a strictly increasing, negative-valued convex function of* $\log x$ *for* $0 < x < 1/\mu$*, and* $f_1(x) \approx -m$ *as* $x \to 1/\mu^-$*. (*m *is the* mass*, defined above.)*
(ii) The function f_2 *is a strictly increasing, convex function of* $\log x$ *for* $x > 1/\mu$*, and satisfies* $0 < f_2(x) \le \log \mu + \log x$*.*

Some, but not all of the above results were previously proved in [35], but these three theorems elegantly capture all that is rigorously known.

In [36] a highly efficient algorithm for enumerating such walks is given. The time required to obtain the number of walks on $L \times M$ rectangles grows exponentially with M and linearly with L. The algorithm is easily generalised to include a step fugacity x. The generalisation to spanning walks is also quite simple. The generalisation to cow-patch patterns is more complicated. Graphs can now have many separate components. Using this algorithm, they calculated $c_n(L)$ for all n for $L \leq 17$. In addition, they computed $C_{18}(1)$ and $C_{19}(1)$.

As noted, it has been proved [34,35] that $\lim_{M\to\infty} C_{M,M}^{\frac{1}{M^2}} = \lambda$ exists. From this it is reasonable to expect, but not a logical consequence, that $R_M = C_{M+1,M+1}/C_{M,M} \sim \lambda^{2M}$. If so, the generating function $\mathcal{R}(x) = \sum_M R_M x^M$ has a radius of convergence $x_c = 1/\lambda^2$, which they estimated using differential approximants [38]. For the crossing problem they found $x_c = 0.32858(5)$, for the spanning problem $x_c = 0.3282(6)$ and for the cow-patch problem $x_c = 0.328574(2)$. It can be proved that these three problems have the same growth constant, so taking the most precise estimate, they obtained $\lambda = 1.744550(5)$.

As well as this estimate, it is possible to obtain rigorous bounds. In [34] it was proved that

Theorem 4. *For each fixed M, $\lim_{L\to\infty} C_{L,M}^{\frac{1}{LM}} = \lambda_M$ exists.*

It similarly follows that $\lim_{M\to\infty} C_{M,M}^{\frac{1}{M^2}} = \lambda$ exists, which was proved rather differently in [35]. In [34] the useful bound $\lambda > \lambda_M^{\frac{M}{M+1}}$ is proved. The above evaluation of λ_2 immediately yields $\lambda > 1.4892\ldots$. Based on exact enumeration, Bousquet-Mélou et al. [36] obtained the exact generating functions $G_3(x)$, $G_4(x)$ and $G_5(x)$. From these, they found the following values: $\lambda_3 = 1.76331\ldots$, $\lambda_4 = 1.75146\ldots$, and $\lambda_5 = 1.74875\ldots$ from which they obtained the bound $\lambda > 1.59321\ldots$.

6.1. Asymptotics

Bousquet-Mélou et al. [36] also considered the exact and asymptotic results for walks crossing a square of length $2L + 2K$. Recall that the shortest walk is of length $2L$. For $K = 0$ the number of such SAW is just $\binom{2L}{L}$. These are so-called ballot numbers. This result is obvious, as there are $2L$ steps in the path, of which L must be in the positive x (and of course positive y) direction. Note that this has the asymptotic expansion

$$\frac{4^L}{\sqrt{L\pi}}(1 - \tfrac{1}{4L} + \tfrac{1}{128L^2} + \tfrac{5}{1024L^3} + \cdots). \tag{42}$$

For $K = 1$ they proved that the number of paths is given by $2L\binom{2L}{L+2}$. This result has the asymptotic expansion

$$\frac{L4^L}{\sqrt{L\pi}}(2 - \frac{33}{4L} + \frac{1345}{64L^2} - \frac{23835}{512L^3} + \cdots). \tag{43}$$

For $K = 2$ they proved that the number of paths is given by

$$\frac{2(2L)!}{L!(L+4)!}(48 + 90L + 8L^2 - 28L^3 - 3L^4 + 4L^5 + L^6) - 4, \tag{44}$$

which has the asymptotic expansion

$$\frac{L^2 4^L}{\sqrt{L\pi}}(2 - \frac{49}{4L} + \frac{2913}{64L^2} + \cdots). \tag{45}$$

For $K = 3$ they found, numerically, that

$$\frac{L^3 4^L}{\sqrt{L\pi}}(\frac{4}{3} - \frac{49}{6L} + \frac{1931 \pm 1}{64L^2} + \cdots), \tag{46}$$

and for $K = 4$ they found the corresponding result

$$\frac{L^4 4^L}{\sqrt{L\pi}}(\frac{2}{3} + \frac{11}{4L} + \cdots). \tag{47}$$

They also gave an heuristic argument for the general form of the leading term in the asymptotic expansion for the case $K = k$. The asymptotic behaviour is dominated by the term $\frac{4^L}{\sqrt{L\pi}}\frac{(2L)^k}{k!}$. They argue that this holds for $k = \mathrm{o}(L^{1/3})$.

Hamiltonian walks (which are necessarily SAW) can only exist on $2L \times 2L$ lattices. For lattices with an odd number of bonds, one site must be missed. A Hamiltonian walk is of length $4L(L+1)$ on a $2L \times 2L$ lattice. The number of such walks grows as τ^{4L^2}, where in [36] it is estimated that $\tau \approx 1.472$. This is about 20% less than λ, the growth constant for all paths. In [34] it is proved that $2^{1/3} \le \tau \le 12^{1/4}$. Numerically, $1.260 \le \tau \le 1.861$. While undoubtedly true, it has not yet been proved that $\lambda > \tau$.

It follows from the three theorems due to Madras, cited above, which hold for general dimensionality $d \ge 2$, that most of the qualitative features described above for the two-dimensional lattice also hold in higher dimension.

Having discussed SAW in random and restricted geometries above, we turn now to other types of randomness, by considering SAW on quasi-random lattices. In exploring the features that change a universality class of a SAW model, it is well known that dimensionality is an important feature, but within a given dimensionality, one can also ask what features determine the universality class? It is known that a change of lattice, among the usual Euclidean Archimedian lattices has no effect on the universality class. In the next two sections we first investigate the effect of a change from a regular to a quasiperiodic lattice, and then in the following section we look at the more drastic change in which the space has negative curvature, and investigate the SAW model on the Poincaré disk.

In summary, we find no evidence of a change of universality class in the former case, but a definite change in the latter case.

7. SELF-AVOIDING WALKS ON QUASIPERIODIC TILINGS

Quasiperiodic tilings are most widely used for the description of quasi-crystals. With appropriate atomic decorations of the vertices, they serve as structure models which explain physical properties of quasi crystals [39]. From a theoretical point of view, they are idealisations of real substances on which the usual models of statistical physics like the Ising model may be studied [40–42]. Quasiperiodic tilings arose before the discovery of quasi-crystals, however, more as an object of aesthetic interest in geometry [43,44].

From a combinatorial point of view, they provide an interesting example of a non-periodic yet structured graph where typical problems of combinatorics like the counting of objects on a lattice become more complex. This is fundamentally different from counting problems on semi-regular lattices, where the underlying translational invariance is still present [45], and also from self-similar graphs, where the self-similarity allows for the solvability of some counting problems.

In the counting problem of n-step SAW on a quasiperiodic tiling, the number depends on the chosen starting point. On a regular lattice, this phenomenon does not occur due to translation invariance. Questions arise, such as if the universal properties of the walks like critical exponents [4] are changed for quasiperiodic tilings, and how different ways of counting affect asymptotic properties. The first question has been investigated for self-avoiding walks (SAWs) and self-avoiding polygons (SAPs) in [46]. Extrapolation of exact enumeration data for a number of quasiperiodic tilings [47,40] indicates that the critical exponents γ for SAWs and α for SAPs are consistent with the corresponding values on regular lattices $\alpha = 1/2$ and $\gamma = 43/32$. In [48], the related problem of SAWs on Penrose random tilings [49] has been studied by Monte Carlo simulations, indicating the same mean square displacement exponent as for regular lattices. The studies [47,40] suffered however from strong finite-size effects due to the relatively short series data available. This is mainly due to the fact that the finite-lattice method [50], being the most successful method known to date for walk enumeration on regular lattices [51,52], cannot easily be applied to this problem, and so to date the exponentially slower method of direct counting has been used. Another reason for the pronounced finite-size behaviour is that the number of walks or loops depends on the chosen starting point. One might suspect that suitable averaging over different starting points reduces these effects, leading to behaviour comparable to the square lattice case.

In [46] a thorough study of this topic was made by utilising three different methods of counting. Whereas the first one depends on a chosen vertex of the tiling, the last two are averages over the whole tiling.

- *Fixed origin walks.* The number of n-step SAW emanating from a given vertex are counted. This number depends on the chosen vertex.

- *Mean number of walks.* Each n-step SAW is weighted by the probability that it occurs in the infinite tiling. For tilings with quasi-crystallographic k-fold symmetries, these probabilities are numbers in the underlying module $\mathbb{Z}[e^{2\pi i/k}]$. This leads to a generating function with non-integer coefficients.

- *Total number of walks.* All translationally inequivalent n-step SAW are counted. These may occur anywhere in the lattice. This number is bigger than the number of fixed origin walks, and by definition, takes into account vertices over the whole tiling.

For self-avoiding polygons, one must distinguish between different fillings of the same loop. In [46] they employed the second and the third method of counting for this problem. The third method has another combinatorial interpretation: The total number of n-step polygons is the number of n-step loops on the tiling, where one counts all possible ways of filling the interior. This may be denoted a *random polygon*. For SAPs, the second method

has been implemented previously [40] in order to obtain the high temperature expansion of the Ising model. The mean number of SAPs up to length $2n = 18$ has been determined on the Ammann-Beenker tiling [53,54] and on the rhombic Penrose tiling [43,55].

Rogers, Richard and Guttmann [46] counted SAWs and SAPs on the Ammann-Beenker tiling and the rhombic Penrose tiling and compared different counting schemes, thereby extending and generalising the previous approaches to counting SAWs [47] and SAPs [40]. Generally speaking, averaging reduces oscillation of data due to finite size effects, providing improved estimates for critical points and critical exponents. Within numerical accuracy, they find it plausible that SAWs on the Ammann-Beenker and on the rhombic Penrose tilings have the same exponents as on the (regular) square lattice. The data for the total number of walks (polygons) gives a different exponent, reflecting the fact that the number of patches grows quadratically with the patch size, in contrast to the regular lattice case [56,57]. The limited SAP data did not allow them to draw decisive conclusions about exponents.

As it is not at all clear how one generates SAW and SAP on these lattices, we describe this in the following subsection.

7.1. Graph generation

Quasiperiodic tilings in $\mathbb{R}^d$ may be obtained by projecting certain subsets of lattices from a higher-dimensional space $\mathbb{R}^n$ into $\mathbb{R}^d$. This is described by a *cut-and-project scheme*, summarised in the following diagram:

$$\begin{array}{ccccc} & \overset{\pi_{||}}{} & & \overset{\pi_{\perp}}{} & \\ E_{||} \simeq \mathbb{R}^d & \longleftarrow & E = \mathbb{R}^n & \longrightarrow & E_{\perp} \simeq \mathbb{R}^m \\ \cup & \underset{1\text{–}1}{\nwarrow} & \cup & \underset{\text{dense}}{\nearrow} & \cup \\ L_{||} = \pi_{||}(L) & & L \text{ lattice} & & W \text{ polytope} \end{array}$$

It consists of a Euclidean vector space E, together with orthogonal projections $\pi_{||}$ and $\pi_{\perp}$. The vector spaces $E_{||} = \pi_{||}(E)$ and $E_{\perp} = \pi_{\perp}(E)$ are called *direct* and *internal* space, respectively. Let $L \subset E$ be a lattice. The projections are such that $\pi_{||}|_L$ is one-to-one and $\pi_{\perp}(L)$ is dense in $E_{\perp}$ (or dense in some subspace of $E_{\perp}$). Let $W \subset E^{\perp}$ be a polytope (or a finite union of polytopes). The set W is also called the *acceptance window*. The set of tiling vertices $\Lambda(W)$ is defined by

$$\Lambda(W) = \{\mathbf{x}_{||} \in L_{||} \,|\, \mathbf{x} \in L \text{ and } \mathbf{x}_{\perp} \in W\}. \tag{48}$$

The edges of the tiling are defined by the following rule: The tiling vertices $\pi_{||}(\mathbf{x})$ and $\pi_{||}(\mathbf{y})$ are adjacent iff the lattice vectors $\mathbf{x}$ and $\mathbf{y}$ are adjacent. For the Ammann-Beenker tiling [53,54], one has $n = 4$ and $d = m = 2$. The lattice is $L = \mathbb{Z}^4$. The projections $\pi_{||}$ and $\pi_{\perp}$ are defined as follows. For $\mathbf{x} \in \mathbb{R}^n$, we set

$$\begin{aligned} \mathbf{x}_{||} &= \begin{pmatrix} 1 & \cos\frac{\pi}{4} & \cos\frac{2\pi}{4} & \cos\frac{3\pi}{4} \\ 0 & \sin\frac{\pi}{4} & \sin\frac{2\pi}{4} & \sin\frac{3\pi}{4} \end{pmatrix} \mathbf{x}, \\ \mathbf{x}_{\perp} &= \begin{pmatrix} 1 & \cos\frac{3\pi}{4} & \cos\frac{6\pi}{4} & \cos\frac{9\pi}{4} \\ 0 & \sin\frac{3\pi}{4} & \sin\frac{6\pi}{4} & \sin\frac{9\pi}{4} \end{pmatrix} \mathbf{x}. \end{aligned} \tag{49}$$

The acceptance window $W \subset \mathbb{R}^m$ is a regular octagon with unit side length centred at the origin, having edges perpendicular to the axes. A typical patch is shown in Figure 2.

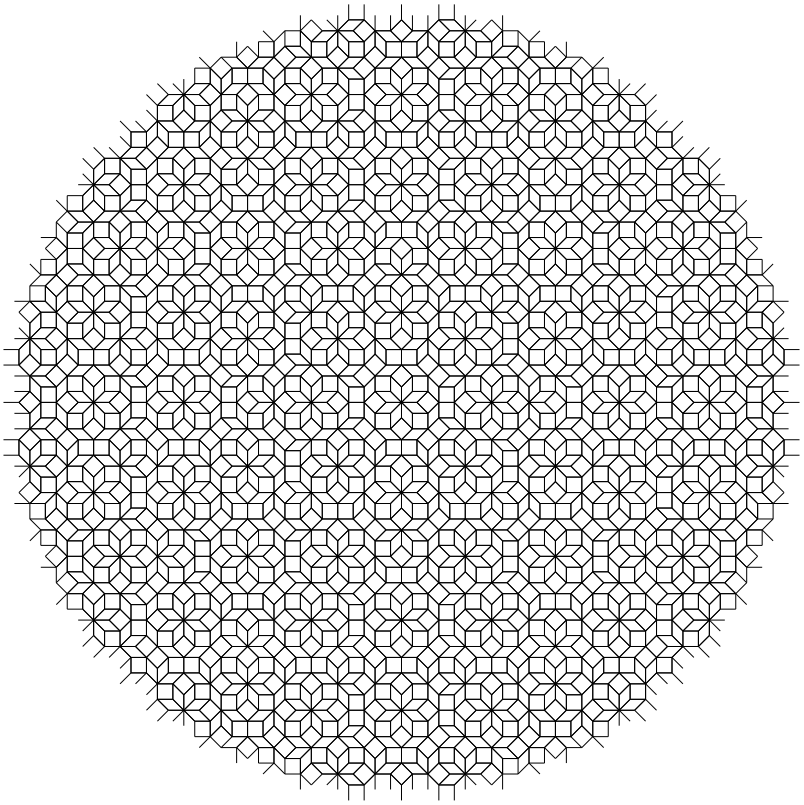

Figure 2. A patch of the Ammann-Beenker tiling.

For the rhombic Penrose tiling [43,55], one has $n = 5$, $d = 2$ and $m = 4$. The lattice is $L = \mathbb{Z}^5$. The projections $\pi_{||}$ and $\pi_\perp$ are, for $\mathbf{x} \in \mathbb{R}^n$, defined by

$$\begin{aligned} \mathbf{x}_{||} &= \begin{pmatrix} 1 & \cos\frac{2\pi}{5} & \cos\frac{4\pi}{5} & \cos\frac{6\pi}{5} & \cos\frac{8\pi}{5} \\ 0 & \sin\frac{2\pi}{5} & \sin\frac{4\pi}{5} & \sin\frac{6\pi}{5} & \sin\frac{8\pi}{5} \end{pmatrix} \mathbf{x}, \\ \mathbf{x}_\perp &= \begin{pmatrix} 1 & \cos\frac{4\pi}{5} & \cos\frac{8\pi}{5} & \cos\frac{12\pi}{5} & \cos\frac{16\pi}{5} \\ 0 & \sin\frac{4\pi}{5} & \sin\frac{8\pi}{5} & \sin\frac{12\pi}{5} & \sin\frac{16\pi}{5} \\ 1 & 1 & 1 & 1 & 1 \end{pmatrix} \mathbf{x}. \end{aligned} \tag{50}$$

The acceptance window $W \subset \mathbb{R}^m$ is made up of four regular pentagons in the planes $\mathbf{x}_{\perp 3} = 0, 1, 2, 3$. The pentagons in the 0 and 3 x_3-planes have unit side length and the others have side length $2\cos\frac{\pi}{5}$. Each pentagon is centred at $\mathbf{x}_{\perp 1} = 0$, $\mathbf{x}_{\perp 2} = 0$. Pentagons 0 and 2 have an edge crossing the positive $\mathbf{x}_{\perp 1}$ axis at right angles while pentagons 1 and 3 are rotated through $\frac{\pi}{5}$. A typical patch is shown in Figure 3.

Note that a more natural embedding of the rhombic Penrose tiling is the root lattice A_4, see also [58], but $\mathbb{Z}^5$ is more convenient for computations. Moreover, the Ammann-

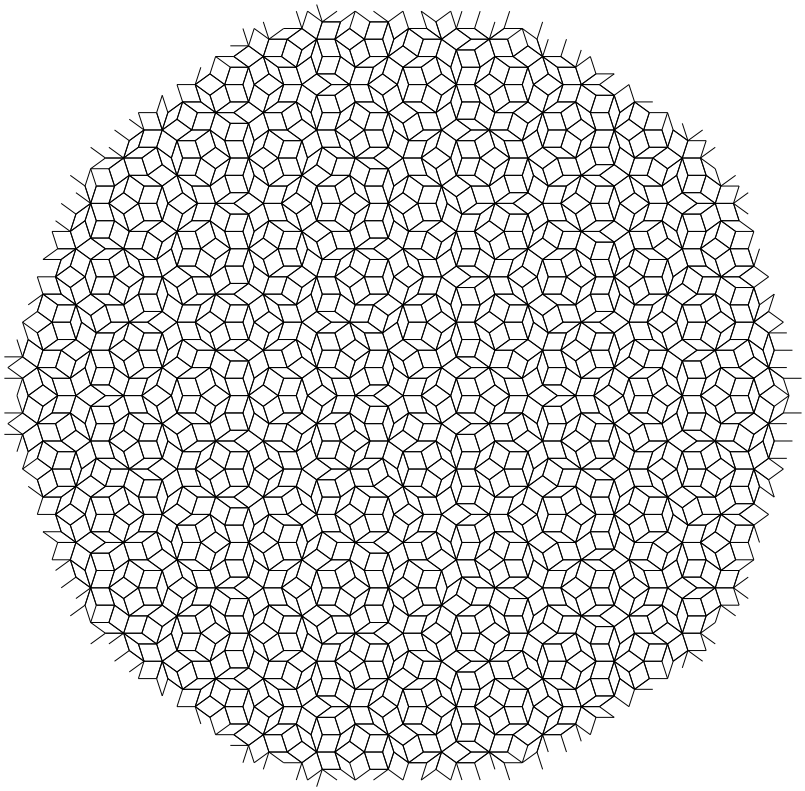

Figure 3. A patch of the rhombic Penrose tiling.

Beenker tiling and the rhombic Penrose tiling may be alternatively defined by inflation rules for their prototiles [59,60].

7.2. Enumeration

The number c_n of translationally inequivalent n-step walks on a regular lattice is clearly independent of the choice of origin vertex. Hence this series is representative of the entire lattice. The enumeration of SAWs on non-periodic tilings introduces complications to the interpretation of the generating function $C(x) = \sum_{n \geq 0} c_n x^n$. This is because the possible origin vertices produce an infinite range of different series $C(x)$. Each origin produces a different series which is representative only of that vertex's immediate neighbourhood in the tiling. As described above, in [46] Rogers et al. adopted three different approaches to enumerating SAWs on quasiperiodic tilings, viz:

- *Fixed origin walks.*
- *Mean number of walks.*
- *Total number of walks.*

7.3. Fixed origin walks

Take a random selection of origin vertices $\mathbf{x} \in L$ (if $\mathbf{x}_\perp \notin W$ the vertex is not a suitable choice and is ignored). For each suitable origin, generate the neighbourhood of the vertex, including all vertices up to some Euclidean distance N away. Two such neighbourhoods are shown in Figure 2 and Figure 3. Enumerate all SAWs from the origin up to length n in the neighbourhood using backtracking [61]. This takes time proportional to the number of walks c_n.

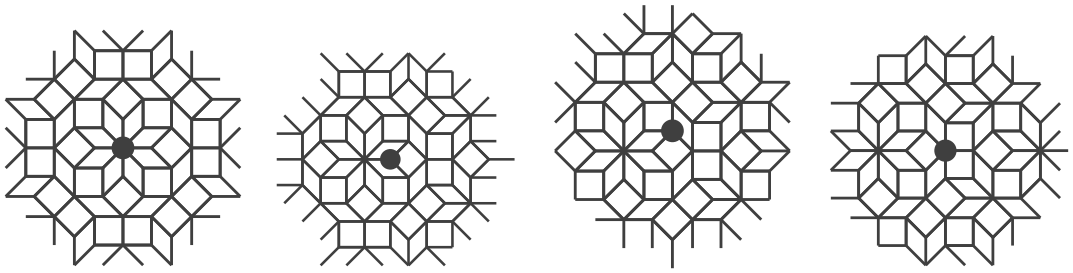

Figure 4. The actual Ammann-Beenker neighbourhoods chosen for the enumerations.

If each of the series in Table 1 and Table 2 showed lattice consistent properties, it would be a good indication that these properties belong to the entire tiling.

n	$\mathbf{x}_\perp = (0,0)$	$\mathbf{x}_\perp = (1,0)$	$\mathbf{x}_\perp = (1-\frac{\sqrt{2}}{2}, \frac{\sqrt{2}}{2})$	$\mathbf{x}_\perp = (1-\sqrt{2}, 0)$
0	1	1	1	1
1	8	3	4	5
2	16	13	12	16
3	48	34	46	42
4	144	108	108	152
5	448	292	374	388
6	1088	952	976	1194
7	3680	2458	3042	3412
8	9584	7746	8330	9678
9	28336	21348	24556	27218
10	82960	61478	68376	79150
11	225408	177230	197820	217562
12	657536	495808	554108	628996
13	1834768	1412152	1576464	1741464
14	5140752	3985706	4400920	4968606
15	14584112	11125408	12531794	13724682
16	40222672	31617786	34541864	39209054
17	114683280	87149372	98846548	107503768
18	313146848	248799302	270221012	306845714
19	896810944	680172768	773046904	840463852
20	2437468000	1943692238	2109562128	2386875508
21	6958267152	5303535884	6011045200	6548653714
22	18981078176	15086983820	16431248782	18500898140
23	53728620912	41295324398	46538635588	50883461478
24	147472084608	116624466842	127704810544	142927122532
25	413887940176			

Table 1
The number of n-step fixed origin SAWs for various starting points $\mathbf{x}_\perp$ in the Ammann-Beenker tiling, with starting point coordinates (x, y) given in the internal space.

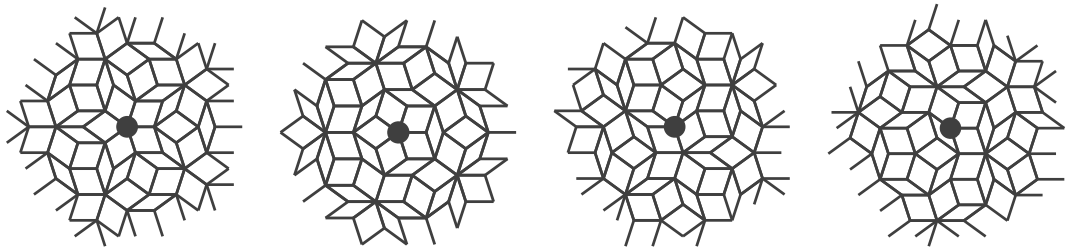

Figure 5. The actual rhombic Penrose neighbourhoods chosen for the enumerations.

n	$\mathbf{x}_\perp = (0,0,1)$	$\mathbf{x}_\perp = (0,0,0)$	$\mathbf{x}_\perp = (0.5,0.5,1)$	$\mathbf{x}_\perp = (0.25,0.5,0)$
0	1	1	1	1
1	5	5	5	4
2	20	10	14	12
3	40	40	50	46
4	160	130	130	112
5	450	310	406	394
6	1170	1140	1177	938
7	4000	2680	3316	3416
8	9480	9360	9723	7866
9	32910	23150	27356	27312
10	76090	72520	77747	66150
11	262250	196980	224102	215924
12	619460	555290	615549	545062
13	2050500	1646990	1812802	1698548
14	5052310	4292010	4869786	4411293
15	15828550	13403280	14455725	13367278
16	41103090	33637420	38524509	35243859
17	121759470	106779600	114089288	105117832
18	331072990	265198150	304434061	279216083
19	937563530	840669610	894584372	825140032
20	2642381430	2092703550	2399386239	2199738033
21	7227151280	6573888100	6988332717	6459329037
22	20931973090	16491425740	18844561759	17267339059
23	55793302330	51185968460	54473434666	50419312152
24	164764171030	129673789110	147471723662	135162732506

Table 2
The number of fixed origin n-step SAWs for various starting points $\mathbf{x}_\perp$ in the rhombic Penrose tiling, with starting point coordinates (x, y, z) given in the internal space.

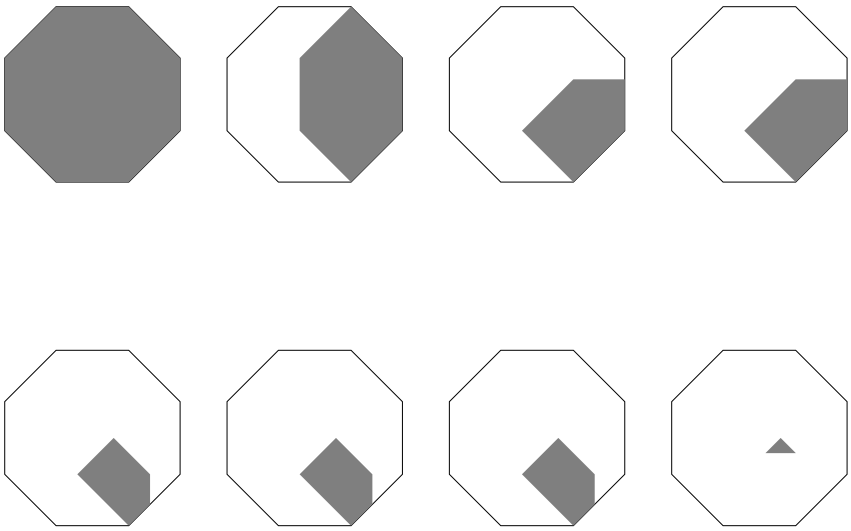

Figure 6. Examples of $W^0 \ldots W^7$ for a particular walk on the Ammann-Beenker tiling.

7.4. Mean number of walks

Given that a pair of vertices from $\Lambda(W)$ are adjacent if and only if they are adjacent in L, one sees that the neighbours of a vertex with image $\mathbf{x}_\perp$ can be found by sequentially adding the $E_\perp$ image of all possible edges in L to $\mathbf{x}_\perp$ and testing if the new points lie in W. If it does the adjacent vertex exists in $\Lambda(W)$. By recursively checking all possible neighbours of a vertex, all possible walks on the lattices will be found.

Given an origin vertex x^0 in $\Lambda(W)$, we know its $E_\perp$ image $x^0_\perp$ must lie somewhere in W, i.e. $x^0_\perp \in W^0 = W$ (W^n is the region $x^0_\perp$ can lie in, given our knowledge of the n steps in the walk). If one takes a step s (with projection $s_\perp$ onto $E_\perp$) to a possible adjacent vertex x^1, then one knows $x^1_\perp = x^0_\perp + s_\perp$. Furthermore if $x^1 \in \Lambda(W)$ is true, then $x^1_\perp \in W$. Hence $W^1 = (W \cap (W^0 + s_\perp)) - s_\perp$. The probability that the step s is possible from a random x^0 is given by the ratio between the areas of W^1 and W.

Extending this to a walk of length n with steps $s^i, i = 1 \ldots n$, $W^k = (W \cap (W^{k-1} + \sum_{i=1}^k s^i_\perp)) - \sum_{i=1}^k s^i_\perp$, the probability of the walk existing is the ratio of the areas of W^n and W. For example, consider the shaded W^i in Figure 6, for the particular walk in the Ammann-Beenker tiling which steps west, south, south-west, north-west, west, north then north. For the Ammann-Beenker tiling, these probabilities are of the form $a + b\lambda$, where $\lambda = 1 + \sqrt{2}$ and $a, b \in \mathbb{Q}$.

Adding the self-avoiding constraint and summing the probabilities results in the expected number of SAWs beginning at a random origin. This process leads to mean numbers of the form $a + b\tau$, where $\tau = (1 + \sqrt{5})/2$ is the golden ratio, and $a, b \in \mathbb{Z}$. The rhombic Penrose tiling also allows steps in ten directions, more than the Ammann-Beenker tiling's eight. These facts combine to allow greater length series to be computed on the Ammann-Beenker tiling.

n	Ammann-Beenker	rhombic Penrose
0	1	1
1	4	4
2	52-16λ	62 -30τ
3	80-16λ	-4 + 28τ
4	444-134λ	914 -488τ
5	1280-380λ	-820 + 732τ
6	4492-1430λ	13842 -7894τ
7	10848-3248λ	-17732 + 12860τ
8	60988-21700λ	173876 -101988τ
9	89800-27036λ	-255784 + 173720τ
10	643248-237732λ	1923078 -1143988τ
11	979776-324200λ	-3149856 + 2073192τ
12	5486960-2043420λ	19566548 -11734706τ
13	10785736-3819788λ	-34951044 + 22612992τ
14	45253532-16927618λ	192557132 -116151274τ
15	110294592-40576780λ	-366912524 + 234803904τ
16	375796808-141368464λ	
17	1058437232-398339560λ	
18	3259350860-1238175678λ	
19	9526156024-3632872284λ	
20	29127575440-11192322668λ	
21	81536068712-31337365980λ	
22	259724099656-100797073134λ	

Table 3
The mean number of n-step SAWs for the Ammann-Beenker tiling and the rhombic Penrose tiling, where $\lambda = 1 + \sqrt{2}$ and $\tau = (1 + \sqrt{5})/2$.

7.5. Total number of walks

Investigating all possible walks as in the mean number of walks method, Rogers et al. [46] counted instead the number of non-zero contributions to the mean value. This counts the number of translationally inequivalent walks with W^n having positive area or, equivalently, the number of translationally inequivalent walks which may occur anywhere in the tiling.

n	Ammann-Beenker	Penrose
0	1	1
1	8	10
2	56	90
3	288	560
4	1280	2800
5	5344	12060
6	20288	48520
7	74192	182000
8	260336	658300
9	892800	2282400
10	2976512	7749440
11	9828256	25634920
12	31758112	83615140
13	101847216	268113660
14	322240144	850895040
15	1012048208	2668534600
16	3147031584	
17	9732815728	
18	29852932384	
19	91182029360	
20	276695822928	
21	836719766336	
22	2516664888416	

Table 4
The total number of n-step SAWs for the Ammann-Beenker tiling and the rhombic Penrose tiling.

7.6. Self-avoiding polygons

A self-avoiding polygon is equivalent to a self-avoiding walk in which the two degree one vertices are adjacent. In the enumeration of self-avoiding polygons, one must distinguish between polygons having, up to a translation, the same boundary but different fillings of the interior. SAPs may be enumerated in the same manner as SAWs.

For the computation of occurrence probabilities of self-avoiding polygon patches, *all* vertices of the patch were taken into account. If the self-avoiding walk patch has n vertices $x^i \in \Lambda(W)$, where $i = 1, \ldots, n$, the acceptance domain is $W^n = \bigcap_i (W - x^i_\perp)$, and the occurrence probability is given by the ratio between the areas of W^n and W, see also [40].

The various sequences were analysed using standard methods of asymptotic analysis of power series expansions as described in [38]. For self-avoiding walks and polygons, it is easy to prove that the limit $\lim_{n\to\infty}(c_n)^{1/n}$ exists by use of concatenation arguments [4]. We assume the usual asymptotic growth of the sequence coefficients c_n, viz:

$$c_n = A x_c^{-n} n^{\gamma-1} \left[1 + \mathcal{O}(n^{-\varepsilon})\right] \qquad (n \to \infty, 0 < \epsilon \leq 1). \tag{51}$$

n	mean number	total number	mean number	total number
2	4	8	4	10
4	8	48	8	80
6	12λ	384	108-48τ	840
8	800-272λ	2960	240-64τ	6480
10	2840-880λ	21600	6192-3364τ	49760
12	28152-9984λ	170256	25584-13248τ	394080
14	47712-9884λ	1322048	179200-95340τ	3087140
16	869600-299392λ	10194720	162976-5440τ	24020160
18	215712+294408λ	79960896	2704140-1067580τ	183529440
20	14980920-3730840λ	618248240		
22	152588920-47048100λ	4726263168		

Table 5
The mean number of n-step SAPs and the total number of SAPs for the Ammann-Beenker tiling (first two columns) and for the rhombic Penrose tiling (last two columns), where $\lambda = 1 + \sqrt{2}$ and $\tau = (1 + \sqrt{5})/2$.

On the square lattice, there is overwhelming evidence [52] of the above asymptotic behaviour with exponent $\gamma = 43/32$. There is however no proof of this assumption. The above assumption results in the following asymptotic growth of the ratios r_n

$$r_n = \frac{c_n}{c_{n-1}} = \frac{1}{x_c}\left[1 + \frac{\gamma - 1}{n} + \mathcal{O}(n^{-1-\varepsilon})\right] \qquad (n \to \infty, 0 < \epsilon \leq 1), \tag{52}$$

which may be used to extrapolate numerical estimates of x_c and γ. Whereas it has been proved for the square lattice that the limit $\lim_{n\to\infty} c_n/c_{n-2}$ exists and coincides with x_c^{-2} [62], a similar statement for the ratios r_n is not known. Indeed, for some lattices, counterexamples are known [63].

Fig. 7 shows a plot of the ratios r_n against $1/n$ for a typical fixed origin Ammann-Beenker walk (full circles) and for the ratios of the mean numbers of Ammann-Beenker walks (large empty circles). Notice that the fixed origin data suffers from dramatic fluctuations, which are smoothed out by averaging, but are still larger than the corresponding square lattice data [52], which is shown in small circles. The oscillating behaviour of the mean number of walks data is due to an additional singularity of the sequence generating function at $x = -x_c$, which, for the case of the square lattice, is well understood due to anti-ferromagnetic ordering [52]. To obtain estimates of x_c and γ, Rogers et al. [46] used the standard method described in [38] and first mapped away the singularity on the negative real axis by an Euler transform and then used Neville-Aitken series extrapolation.

They also used the method of differential approximants (DAs) [38]. The underlying idea is to fit a linear differential equation with polynomial coefficients to the generating function of the sequence, truncated at some order n_0. In Table 6 the results for the DA analysis are listed.

The estimate using the data for the mean number of walks yields the most precise estimates, which are, however, one order of magnitude in accuracy worse than the corresponding estimates for square lattice SAWs, given such a series of equal length.

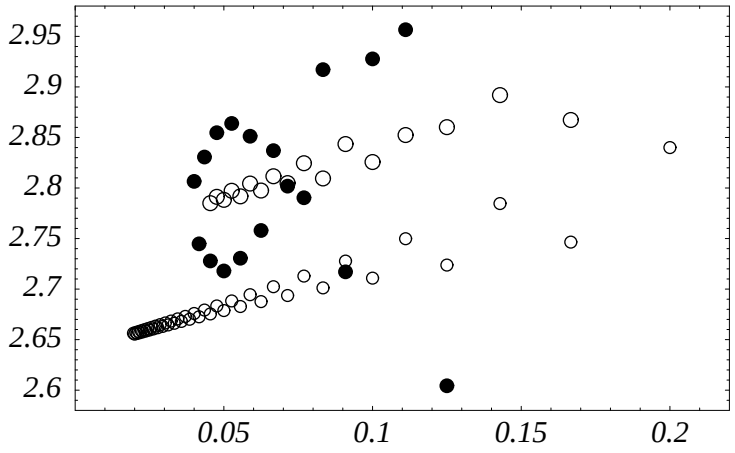

Figure 7. Ratio plot of c_n/c_{n-1} against $1/n$ for fixed origin (full circles) and mean number (large empty circles) Ammann-Beenker SAWs. The square lattice SAW data is plotted in small circles for comparison.

	mean no.	$(0,0)$	$(1-\frac{\sqrt{2}}{2},\frac{\sqrt{2}}{2})$	$(1,0)$	$(1-\sqrt{2},0)$
x_c	0.36414(18)	0.3659(14)	0.3644(13)	0.3644(21)	0.3657(16)
γ	1.325(19)	1.45(16)	1.30(14)	1.32(17)	1.46(17)

Table 6
Estimates of x_c and γ for Ammann-Beenker SAWs. Numbers in brackets denote the uncertainty in the last two digits.

An analysis of the total number of SAWs on the Ammann-Beenker tiling using first order DAs yielded $x_c = 0.3647(33)$ and $\gamma = 3.14(37)$. Whereas the critical point estimate is consistent with the previous analysis, the exponent estimate deviates from the value of $43/32 = 1.34375$ for fixed origin SAWs or the mean number of SAWs. This phenomenon reflects the fact that the number of Ammann-Beenker patches of radius r grows asymptotically as r^2. (More generally, for aperiodic Delone sets in $\mathbb{R}^d$ described by a primitive substitution matrix, the number $N(r)$ of patches of radius r grows like $N(r) \simeq r^d$ [57,56].) Since the SAW has fractal dimension $4/3$, we expect an asymptotic increase of the number of SAWs by $n^{2\nu}$, where $\nu = 3/4$. Thus $\gamma = 43/32 + 2\nu = 2.84375$. The above estimate is consistent with this value.

The analysis of SAP data followed the same lines. However, the estimates suffered from large finite size errors due to the low number (11) of available coefficients. First order differential approximants for the mean number of SAPs yielded $x_c = 0.3688(41)$.

For the critical exponent $\alpha = 2 + \gamma$, one expects by universality that $\alpha = 1/2$, being the believed exact value for the square lattice (and numerically confirmed to very high precision [64]). Due to lack of data it is not possible to give estimates of critical exponents. An analysis of the total number of SAPs on the Ammann-Beenker tiling using first order DAs yields $x_c = 0.3587(15)$.

The above analysis has also been applied to the rhombic Penrose tiling data. That data displays qualitatively the same finite size behaviour as the Ammann-Beenker tiling data. In Table 7 estimates of x_c and γ obtained by analysing first order differential approximants are given.

	mean no.	$(0,0,0)$	$(0,0,1)$	$(0.25,0.5,0)$	$(0.5,0.5,1)$
x_c	0.36322(29)	0.3621(12)	0.3613(16)	0.36248(83)	0.36347(51)
γ	1.333(26)	1.28(14)	1.19(22)	1.303(83)	1.387(62)

Table 7
Estimates of x_c and γ for Penrose SAWs. Numbers in brackets denote the uncertainty in the last two digits.

An analysis of the total number of SAWs on the rhombic Penrose tiling using first order DAs yielded $x_c = 0.3638(31)$ and $\gamma = 2.77(21)$. The estimate of the critical point is consistent with the estimates from the other methods of counting. For the critical exponent, one again expects a value of $\gamma = 43/32 + 2\nu = 2.84375$, which agrees with the extrapolation within numerical accuracy.

For the analysis of SAP data, only 9 series coefficients are available. First order differential approximants for the mean number of SAPs yielded $x_c = 0.372(11)$. An analysis of the total number of SAPs on the rhombic Penrose tiling using first order DAs yielded $x_c = 0.3590(22)$. Again, due to lack of data, it is not possible to obtain reasonable estimates for the critical exponent α.

In summary, it turns out that averaging with respect to the occurrence probability in the whole tiling leads to the best estimates of the critical parameters, whereas data produced by fixing an origin leads to strong finite size oscillations. The results support the universality hypothesis that the critical exponents appear to be the same as for the square lattice, within confidence limits. For the total number of walks (polygons) a new exponent was found, reflecting the polynomial complexity of the number of patches of the underlying tiling.

On a mathematically rigorous level, it may be possible to show the equality of the critical points for SAPs and SAWs on quasiperiodic tilings by appropriately modifying the existing proofs for the hypercubic lattice [68]. Furthermore, it would be interesting to carry out an analysis to determine if random walk behaviour can be proved for dimensions greater than four [4].

8. SELF-AVOIDING WALKS AND POLYGONS ON HYPERBOLIC LATTICES

In two Euclidean dimensions, if we require that every site and every bond of a lattice be equivalent, there are only three possible choices. The square, triangular or honeycomb lattice. On the Poincaré disk, a space with negative curvature, there are infinitely many possibilities.

We wish to construct lattices with equilateral faces and given co-ordination number. The formal geometric construction is succinctly given by Rietman, Nienhuis and Oitmaa

[65] and we quote: "These lattices can be embedded in a homogeneous two dimensional space with constant Ricci curvature. When the curvature is positive, this is the sphere S^2. After Reimann projection $z = x + iy = e^{i\phi} \tan \frac{\theta}{2}$ this becomes the plane with the metric $g_{\mu\nu}(x, y) = \frac{\delta_{\mu\nu}}{(1+z\overline{z})^2}$. When the curvature $R = 0$ we simply have the Euclidean plane with the metric $g_{\mu\nu}(x, y) = \delta_{\mu nu}$. When the curvature is negative we may choose the hyperboloid embedded in a $2 + 1$-dimensional Minkowski space, given by

$$X^2 + Y^2 - Z^2 = -\frac{1}{4}, \; Z \geq \frac{1}{2}. \tag{53}$$

This hyperboloid can be parameterized with coordinates $\psi \in [0, \infty)$, $\phi \in [0, 2\pi)$: $X = \sinh \psi \cos \phi/2$, $Y = \sinh \psi \sin \phi/2$, $Y = \cosh \psi$, and in terms of $z = x + iy = e^{i\phi} \tan \frac{\psi}{2}$ it becomes the circular disc $|z| < 1$ with metric $g_{\mu\nu}(x, y) = \frac{\delta_{\mu\nu}}{(1+z\overline{z})^2}$. The geodesics of this metric are circular arcs (in the flat metric) orthogonal to the circle at infinity, $|z| = 1$. The distance between two points P_1 and P_2 is given by

$$d(P_1, P_2) = \text{arctanh}|\frac{z_1 - z_2}{1 - z_1\overline{z_2}}|''. \tag{54}$$

Note that one is not restricted to the unit disk, though that is the geometry utilised by Swierczak and Guttmann [66] in their study of SAW on the hyperbolic lattices. A conformal mapping would enable geometries other than the unit disk to be considered.

Hyperbolic lattices are characterised by two integers, both greater than 2. One is the number of neighbours of each vertex, v, and the other is the number of sides of each face, denoted f. Lattices are described by the ordered pair (f, v). Another, equivalent, view is that the lattice consists of f-gons, with v of them meeting at each vertex. Such a lattice can be embedded in the sphere, plane or hyperboloid whenever $(v - 2)(f - 2)$ is, respectively, less than 4, equal to 4 and greater than 4. Thus the familiar Euclidean triangular, square and hexagonal lattices are, in this notation, the $(3, 6)$, the $(4, 4)$ and the $(6, 3)$ lattices respectively. There are five possible lattices on the sphere, corresponding to the five Platonic solids. For example, the $(3, 3)$ lattice is the tetrahedron.

The construction of the hyperlattices is rather subtle. As the boundary of a finite section of the lattice contains a finite fraction of the vertices in the finite section, the usual concept of thermodynamic limit becomes rather suspect. In fact, as we increase the "size" of the lattice, the surface to volume ratio remains non-zero, unlike Euclidean lattices, where this quantity vanishes. This is reminiscent of a Cayley tree, and from this observation alone it should not be too surprising that one observes "mean-field" type exponents, as this is the usual manifestation of this "infinite-dimensional" characteristic. From an algebraic viewpoint, the symmetry group of the lattice is generated by two rotational elements. One is a rotation about a given lattice point by $2\pi/v$, and the other is a rotation about the centre of an adjacent face by $2\pi/f$. The group generated by these two operations is a subgroup of the group of isometries of the unit disc in the complex plane, notably the projective group $PSU(1, 1) = SU(1, 1)/\{I, -I\}$. Further details of the group, and group action, can be found in [65].

In [66] both SAW and SAP on the $\{3, 7\}$, the $\{5, 5\}$ and the $\{6, 3\}$ lattices were investigated. In addition, an irregular hyperbolic lattice, denoted $T(2, 3, 7)$ was studied. This

last lattice is a triangulation of the $\{8,4\}$ lattice, in which each octagon is triangulated with 16 triangles, having a common vertex at the centre of the octagon. Enumeration was done by backtracking. In backtracking algorithms on Euclidean lattices, the only problem is speed. Memory demands are minimal. As the algorithm is of exponential complexity, it is that which limits progress. When enumerating on hyperbolic lattices, one has the additional problem of exponential growth in memory requirements. Two strategies to limit this problem are discussed in [66].

For all lattices, series analysis yielded a simple pole as the singularity of the SAW generating function. This is of course different to the Euclidean situation, where the corresponding exponent $\gamma = \frac{43}{32}$. Furthermore, the growth constant for SAW and SAPs for a given lattice is different. Surprisingly, the *exponent* for SAP appears to be the same as for Euclidean lattices, that is $\alpha = \frac{1}{2}$. For the $\{6,3\}$ lattice it was possible to obtain an exact solution. This lattice has a tree-like dual structure, which accounts for the solvability. For SAP on this lattice the generating function was found to be

$$P(x) = \frac{1 - 2x^4 - \sqrt{(1-4x^4)}}{2x^3} = x^5 + 2x^9 + 5x^{13} + \ldots .$$

This is immediately recognisable as the generating function for Catalan numbers, $C_n = \frac{1}{n+1}\binom{2n}{n}$. Thus the connective constant is $\mu_p = 1/\sqrt{2}$, and $\alpha = 1/2$. For SAW the generating function is of a similar form, viz:

$$C(x) = \frac{A(x) + B(x)\sqrt{(1-4x^4)}}{x^6 C(x)} = 1 + 3x + 6x^2 + 12x^3 + 24x^4 + \ldots ,$$

where $A(x)$, $B(x)$ and $C(x)$ are polynomials of degree 12, 8 and 5 respectively. The growth constant is in this case given by a zero of the denominator polynomial, rather than by the branch point of the numerator, as was the case for SAPs. In [66] the value $x_c = 1/\mu = 0.513839377\ldots$ is given, which, as can be seen, is greater than the corresponding result for SAP. The origin of the simple pole singularity is also clear. For the sake of completeness, we remark that in [65] similar results for the Ising model on a hyperbolic lattice were obtained, while in [67] considerable progress is made in understanding many of the strange properties of SAW, and indeed percolation, on such lattices.

9. BIOLOGICAL MODELS: SAW AS MODELS OF DNA

By constraining self avoiding walks in various geometries, and introducing interactions by appropriate fugacities, such SAW turn out to be useful in modelling a surprising variety of biological situations. In this section we will consider just three.

One of the first, historically, is the modelling of the denaturation of DNA. When a solution of DNA is heated, the double stranded molecules denature into single strands. In this process, "looping out" of AT rich regions of the DNA segments first occurs, followed eventually by separation of the two strands as the paired GC segments denature. This *denaturation* process corresponds to a phase transition [69].

A simple model of this DNA denaturation transition was introduced in 1966 by Poland and Scheraga [70,71] (hereinafter referred to as PS) and refined by Fisher [72,73]. The model consists of an alternating sequence (chain) of straight paths and loops, which

idealize denaturing DNA, as a sequence of double stranded and single stranded molecules. An attractive energy is associated with paths. Interactions between the different parts of a chain and, more generally, all details regarding real DNA such as chemical composition, stiffness or torsion, are ignored. It was found that the phase transition is determined by the critical exponent c of the underlying loop class. Due to the tractability of the problem of random loops, that version of the problem was initially studied by PS [71]. The model displays a continuous phase transition in both two and three dimensions. It was argued by Fisher [72] that replacing random loops by self-avoiding loops, suggested as a more realistic representation accounting for excluded volume effects within each loop, sharpens the transition, but does not change its order. We shall investigate this particular model in a little more detail below.

Another early example of a biological problem modelled by SAW—or in this case SAP, was the study of *vesicles* by Leibler and Fisher, [74], Fisher et al. [75] and Banavar et al. [76]. A vesicle is a biological object such as a blood cell whose behaviour is mediated by pressure. If the internal pressure exceeds the external pressure the cell will be inflated, whereas in the opposite situation it will be collapsed. Clearly, there will be a phase transition that occurs at a critical value of the pressure. Early series studies were largely restricted to two dimensions, the cell was modelled by a two-dimensional SAP, and the pressure induced phase transition was mediated by associating a fugacity with the enclosed area. Thus by varying this fugacity, polygon shapes of minimal area, which are long and thin, could be achieved, as could those of maximal area, which are effectively square. We will consider this problem in a little more detail below.

Our third and final example is the use of SAW to model the micromanipulation of polymer molecules, particularly DNA, attached to a surface. In this situation, optical tweezers [77,78] are used to pull the adsorbed biological molecule from the surface. This force is applied perpendicular to the adsorbing surface and will favour desorption. It is reasonable to expect some sort of a phase transition. At low levels of the force, the polymer remains adsorbed, but at higher levels it will be desorbed. There will be a temperature dependent force $f_c(T)$ between these two states. The shape of the force-temperature curve is of considerable interest, and can be considered a phase boundary in the $T - f$ plane. This can be modelled by a SAW, tethered to a wall, with a fugacity associated with nearest-neighbour bonds, subject to a force perpendicular to the wall, as shown in the figure below.

9.1. The DNA denaturation transition

With the advent of efficient computers, it has recently been possible to simulate analytically intractable models extending the PS class, which are assumed to be more realistic representations of the biological problem. One of these is a model of two self-avoiding and mutually avoiding walks, with an attractive interaction between the different walks at corresponding positions in each walk [79–82]. The model exhibits a first order phase transition in two and three dimensions. The critical properties of the model are described by an exponent c' related to the loop length distribution [83–85,80–82], see also Fisher's review article [73]. For PS models, this exponent coincides with the loop class exponent c if $1 < c < 2$. Within a refined model, where different binding energies for base pairs and stiffness are taken into account, the exponent c' seems to be largely independent of

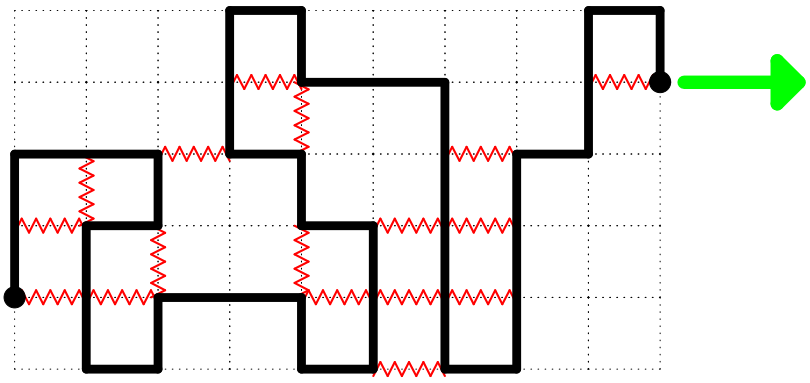

Figure 8. A SAW model of a polymer subject to an elongational force.

the specific DNA sequence and of the stiffness of paired walk segments corresponding to double stranded DNA parts [80]. There are, however, no simulations of melting curves for known DNA sequences which are compared to experimental curves for this model.

An approximate analytic derivation of the exponent related to this model was given by Kafri et al. [83–85] using the theory of polymer networks. They estimated the excluded volume effect arising from the interaction between a single loop and two attached walks. This approach (refined recently [81]) yields an approximation of the loop length distribution exponent c', which agrees well with simulation results of interacting self-avoiding walk pairs [80–82]. There is a recent debate about the relevance of this approximation to real DNA [86]. The polymer network approach, as initiated previously [83], led to a number of related applications [84,85,81,87,88].

Some care needs to be taken in studying the literature on this problem, which may be misleading. This is discussed in considerable detail in Richard and Guttmann [89]. Loop classes discussed in the early approaches [71,72] are classes of *rooted* loops and lead to chains which are not self-avoiding. This seems unsatisfactory from a biological point of view, since real DNA is self-avoiding. Secondly, the common view holds that PS models with self-avoiding loops cannot display a first order transition in two or three dimensions. In fact, this view led to extending the PS class [79,83–85] in order to find a model with a first order transition. However this view is incorrect, as demonstrated [89] by a self-avoiding PS model with self-avoiding loops. Thirdly, the two exponents c and c', extracted from different expressions as described above, are used in the literature without distinction, although there are subtle differences.

In [79] a SAW model of this transition was introduced. Causo et al. [79] considered pairs of SAW on the simple cubic lattice, with a common origin, which are allowed to overlap only at the same monomer position along each chain. That is to say, if one numbers the monomers from the common origin $0, 1, 2, \ldots i, \ldots n$, the two chains are mutually and individually self-avoiding except possibly where site i of the first monomer coincides with site i of the second monomer. Such overlaps are encouraged by a fugacity ϵ, associated with such contacts. As the temperature increases, there is a transition temperature T_m above

which the entropic advantage in breaking such bonds overcomes the attractive energy. From extensive simulations, it was concluded [79] that the transition is first order, as the energy density at the transition was found to be discontinuous.

9.2. Poland-Scheraga models: general formalism

Consider a discrete model, defined on the hypercubic lattice $\mathbb{Z}^d$. Double stranded DNA segments are modeled by paths, and single stranded DNA segments are modeled by loops on the edges of the lattice. Each loop is assumed to have two marked vertices to indicate where paths are attached. Any alternating sequence of paths and (marked) loops is called a *chain*. A *PS model* consists of all chains obtained by concatenation of paths and loops from a given path class and a given loop class, where the initial segment and the final segment of a chain are both paths. Note that, in general, such chains are not self-avoiding, in contrast to real DNA. Self-avoidance may be violated by paths, by loops, or by the way segments are concatenated. A chain is called *segment-avoiding* if there are no overlaps, i.e., every two non-neighboring segments have no vertex in common, and every two neighboring segments have exactly the marked vertex in common. We call a PS model *self-avoiding* if paths and loops are self-avoiding and if all chains of the model are segment-avoiding.

The requirement of self-avoidance restricts the admissible path classes and loop classes. A simple subclass of self-avoiding PS models are directed PS models: We call a chain *directed* if there is a preferred direction such that the order of the chain segments induces the same order on the vertex coordinates (w.r.t. the preferred direction), for each pair of vertices taken from two different chain segments. Such chains are then segment-avoiding. We call a PS model *directed* if paths, loops and chains are directed.

For a given PS model, let $z_{m,n}$ denote the number of chain configurations with m contacts and length n. The generating function is defined by

$$Z(x,w) = \sum_{m,n} z_{m,n} w^m x^n, \tag{55}$$

where the fugacity x is conjugate to the chain length n. The Boltzmann factor $w = e^{-E/kT}$ takes into account the attractive interaction (achieved by setting the energy $E < 0$) between bonds. T is the temperature, and k is Boltzmann's constant. Over the relevant temperature range $0 < T < \infty$, we have $\infty > w > 1$. Note that there is no interaction between different segments in a chain.

The generating function $Z(x,w)$ can be expressed in terms of the generating functions for paths $V(x)$ and loops $U(x)$. These are

$$V(x) = \sum_{n=0}^{\infty} b_n x^n, \qquad U(x) = \sum_{n=1}^{\infty} p_{2n} x^n, \tag{56}$$

where b_n is the number of paths of length n, and p_{2n} is the corresponding number of loops. Due to the chain structure, one gets a geometric series in $V(wx)U(x)$,

$$Z(x,w) = \frac{V(wx)}{1 - U(x)V(wx)} = \sum_{n=1}^{\infty} Z_n(w) x^n. \tag{57}$$

Since we want to analyze phase transitions of the model, which can only occur in the infinite system, we define the free energy of the model as

$$f(w) = \lim_{n\to\infty} \frac{1}{n} \log Z_n(w) = -\log x_c(w), \tag{58}$$

where, for fixed w, $x_c(w)$ is the radius of convergence of $Z(x, w)$. Concatenation arguments and supermultiplicative inequalities can be used to show that the free energy exists [90]. We will alternatively investigate properties of the free energy in terms of the generating functions for paths and loops. It is instructive to consider an exactly solvable model, which is provided by the following fully directed model.

9.3. Fully directed walks and loops

This directed model consists of fully directed walks for the paths in the chain. These are clearly self-avoiding, and only take steps in positive directions. The corresponding loops are staircase polygons, which consist of two fully directed walks, which do not intersect or touch, but have a common starting point and end point. Paths are attached to these points. We distinguish the two strands of a loop.

In $d = 2$, the generating functions for paths and marked loops are [90]

$$V(x) = \frac{1}{1-2x}, \qquad U(x) = 1 - 2x - \sqrt{1-4x}. \tag{59}$$

$U(x)$ is twice the generating function of staircase polygons. The loop class exponent is $c = 3/2$. The generating functions V and U have critical points $x_V = 1/2$, $x_U = 1/4$ and $w_c = 1$, i.e., a phase transition occurs at $T = \infty$. (If the empty path would not be allowed, a phase transition would occur at a finite temperature). The free energy $f(w)$ is given by

$$f(w) = \log\left(\frac{2(w-1)^2}{\sqrt{1+(w-1)^2}-1}\right) \qquad (1 \le w < \infty). \tag{60}$$

The fraction of shared bonds follows as

$$\theta(w) = \frac{2w}{w-1} \frac{\sqrt{1+(w-1)^2}-1-(w-1)^2/2}{1+(w-1)^2-\sqrt{1+(w-1)^2}} \qquad (1 \le w < \infty), \tag{61}$$

which approaches zero linearly in $w-1$. The asymptotic behavior of $Z_n(w)$ about $w = 1$ is given by

$$Z_n(w) \sim \frac{4^{n-1}}{n^{1/2}} h_{\sqrt{n}/8}(w-1) \qquad (n \to \infty,\ w \to 1^+), \tag{62}$$

uniformly in w, where $h_a(x) = \frac{1}{\sqrt{\pi}} + axe^{(ax)^2}(1+\mathrm{erf}(ax))$ and $\mathrm{erf}(x)$ is the error function.

As shown in [89], this PS model of fully directed walks and loops is exactly solvable in arbitrary dimension. The phase transition is found to be first order for $d \ge 6$, to have a continuous phase transition in dimensions $2 \le d \le 5$, and to occur at finite temperature in $d \ge 4$ only.

Since the critical behavior of PS models is essentially determined by the properties of loops, PS [70,71], and later Fisher [72], were led to consider various loop classes (together with straight paths for the double stranded segments). Whereas PS analyzed loop classes derived from random walks, Fisher considered loop classes derived from self-avoiding walks.

9.4. Loops and walks

An oriented, rooted loop of length n is a walk of length $n-1$, whose starting point and end point are lattice nearest neighbors. We identify such loops if they have the same shape, i.e., if they are equal up to a translation, possibly followed by a change of orientation. These objects we call unrooted, unoriented loops, or simply loops. Each loop of length n has at most $2n$ corresponding walks. If the walks are self-avoiding, each loop has exactly $2n$ corresponding walks. The number of loops of length n is denoted by p_n. For example, for self-avoiding loops on $\mathbb{Z}^2$ we have $p_4 = 1$ and $p_6 = 2$. For a given class of walks, the above description defines the corresponding (unmarked) loop class. Within a chain structure, two paths are attached to each loop. Different choices for attachment positions increase the number of (marked) loop configurations to $\widetilde{p}_n \geq p_n$. If we assume the DNA condition that the two paths attached to a loop bisect it into pieces of equal length, then the number of possible attachments of two paths to a loop of length n is less than or equal to $2n$. (We distinguish the two strands of a marked loop). PS and Fisher consider classes of oriented rooted loops. Self-avoiding oriented rooted loops can be interpreted as loops with $2n$ possible attachment positions of paths to a loop of length n. A similar interpretation for oriented rooted random loops is not obvious. We stress that these loop classes result in chains which are not segment-avoiding, as paths will intersect the loops. Both models cannot therefore represent real (self-avoiding) DNA.

9.5. Oriented rooted random loops

The first simple example of loops, discussed by PS [71], is that of oriented rooted random loops derived from random walks. Random walks on $\mathbb{Z}^d$ have the generating function $V_d(x) = 1/(1-2dx)$. The asymptotic behavior of the number of oriented rooted random loops of length $2n$ is given [4] (Appendix A) by

$$\widetilde{p}_{2n} \sim A(2d)^{2n}(2n)^{-d/2} \qquad (n \to \infty). \tag{63}$$

This implies no phase transition in $d = 2$ and a continuous phase transition in $d = 3$.

The PS results led to the question [72] whether accounting for excluded volume effects within a loop increases the loop class exponent c, which might change the order of the phase transition. This led to considering *self-avoiding loops*, which are loops derived from self-avoiding walks. By definition, the self-avoiding loop class fully accounts for excluded volume interactions within a loop. In $d = 3$, self-avoiding loops of length $n \geq 24$ may be knotted. Fisher considered oriented rooted loops $\widetilde{p}_{2n} = 4np_{2n}$. Their loop class exponent c, $\widetilde{p}_{2n} \sim B\mu_d^n n^{-c}$, is related to the mean square displacement exponent ν of self-avoiding walks by the hyperscaling relation $c = d\nu$. For unknotted self-avoiding loops, which is the preferable model from a biological point of view, it has been proved [32] that the exponential growth constant is strictly less than that of all self-avoiding loops, while the exponent (if it exists) is expected to coincide with that of all self-avoiding loops.

Fisher concluded that the above values of the loop class exponent c imply a continuous phase transition in $d = 2$ and $d = 3$. In [89] it is shown that the phase transition condition is satisfied in both $d = 2$ and in $d = 3$ for the case when the double stranded segments are treated as straight paths. Note that in $d = 2$, self-avoiding walks as paths will result in no phase transition.

The previously discussed PS models are not fully self-avoiding, in that the chains are not mutually avoiding. Using SAW for walks, a PS model with segment-avoiding chains may be defined as follows: Take only those walks with extremal first and last vertex. That is to say, if $v(0), v(1), \ldots, v(n)$ are the vertices of an n-step walk v, this walk is taken as a path iff $v_x(0) < v_x(i) < v_x(n)$ for all $1 < i < n$. Such walks are *bridges* [4] (Sec. 1.2), whose last step is in the x-direction. For (unmarked) loops, take loops derived from the walks, that is, SAP. Marking of the loops may be achieved in different ways. To this end, consider for a given loop the sets A_l (A_r) of vertices of smallest (largest) x-coordinate. We distinguish four different types of marking: complete marking (with DNA constraint), where we mark a loop at all vertex pairs from A_l and A_r (whenever the DNA condition is satisfied), and unique marking (with DNA constraint), where we only mark a loop at a single vertex pair, for example the bottom vertex and the top vertex in a lexicographic ordering (if they satisfy the DNA condition).

Unique marking would then imply $\widetilde{p}_n = 2p_n$ (we distinguish the two strands of a marked loop) and hence increase the previous exponents by one. Hence, such a PS model displays a first order transition with $c = 5/2$ in $d = 2$ and with $c = 2.7631(18)$ in $d = 3$. Unique marking with the DNA constraint results in $\widetilde{p}_n \leq 2p_n$. If we assume that the exponential growth constant for marked self-avoiding loops is given by the usual SAP growth constant, this implies a critical exponent c greater or equal to the model with unique marking, i.e., a first order phase transition in $d = 2$ and $d = 3$. For complete marking, we have $2p_n \leq \widetilde{p}_n \leq 2np_n$, which rules out a decrease of c by more than one. However we expect that the number of possible markings is of order 1 as $n \to \infty$, and so c remains unchanged, and the model again displays a first order phase transition. Similar considerations apply for the case of complete marking with DNA constraint.

In summary, as we have shown in brief, and as shown in more detail in [89], a self-avoiding PS model (with unique marking, with self-avoiding bridges and (unrooted) self-avoiding loops) as defined above yields a first order phase transition in both $d = 2$ and $d = 3$.

For the presumably more realistic model of pairs of interacting self-avoiding walks [79,83–85,80–82], the results of [89] suggest an interpretation of excluded volume effects, which complements the common one [83–85]. The self-avoiding PS models discussed above correctly account for excluded volume effects within a loop, but overestimate excluded volume effects between different segments of a chain, due to their directed chain structure. Since this leads to a first order phase transition in $d = 2$ and $d = 3$, one can conclude that the relaxation of excluded volume effects between different segments of the chain does not change the nature of the transition.

The simpler, directed model displays a first order phase transition in $d = 2$, but such models seem to be of limited relevance to the biological problem due to their directed structure and other limitations.

In conclusion, the question of the mechanisms applying in real DNA which are respon-

sible for the denaturation process and which explain multistep behavior as observed in melting curves, are still far from being satisfactorily answered in our opinion, though models based on SAW and SAP still seem to be the most appropriate way to study this important problem.

9.6. Vesicles collapse

In modelling vesicle collapse by SAP, let $p_m(n)$ be the number of SAP per site on an infinite lattice, with perimeter m enclosing area n. In [75] it was proved that the free energy

$$\lim_{m\to\infty} \frac{1}{m} \log \sum_n p_{m,n} q^n := \kappa(q) \tag{64}$$

exists and is finite for all values of the fugacity $q \leq 1$. Further, $\kappa(q)$ is log-convex and continuous for these values of y and is infinite for $y > 1$.

In terms of the natural two-variable generating function

$$P(x,q) = \sum_{x,q} p_{m,n} x^m q^n, \tag{65}$$

it was further proved that for $q < 1$, $P(x,q)$ converges for $x < \mathrm{e}^{-\kappa(q)}$, while for $q > 1$, $P(x,q)$ converges only for $x = 0$. The expected phase diagram is shown in figure 9 below.

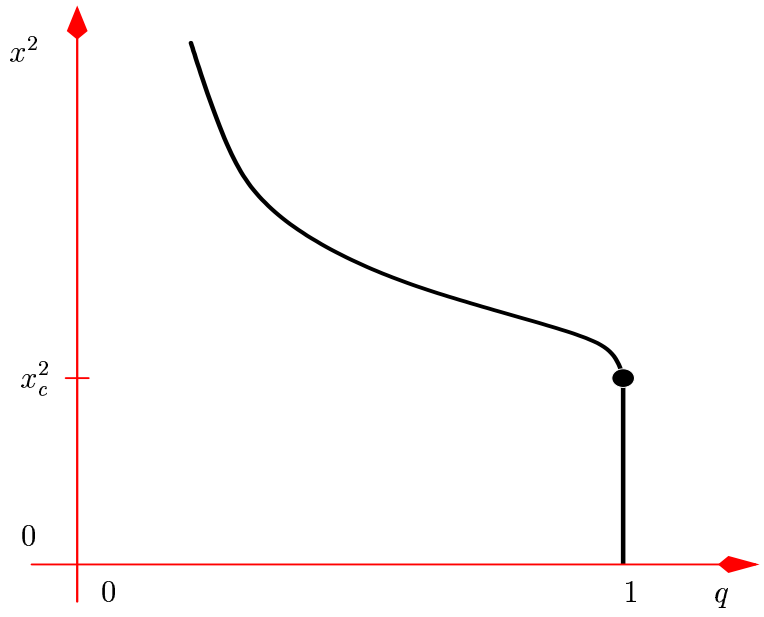

Figure 9. The phase diagram showing the phase boundary $x_c(q)$.

In the region below the phase boundary, the polygons are ramified objects, closely resembling branched polymers. That is to say, they are collapsed and string-like. As q

approaches unity, they fill out more, and become less string-like. At $q = 1$ one has pure SAP. For $q > 1$ the polygons become "fat", and approximate squares, with their average area scaling as the square of their perimeter. In [75] rigorous upper and lower bounds to the shape of the phase boundary were found, and the locus of the actual phase boundary was found numerically from extrapolation of SAP enumerations by area and perimeter.

In the extended phase $q = 1$, the mean area of polygons $\langle a \rangle_m$ of perimeter m grows asymptotically like $m^{3/2}$, whereas it grows like m in the deflated phase $q < 1$. It can be shown that in the limit $q \to 0$ the generating function is dominated by polygons of minimal area. Since for SAPs these polygons may be viewed as branched polymers, the phase $q < 1$ is also referred to as the *branched polymer phase*. This change of asymptotic behaviour is reflected in the singular behaviour of the perimeter and area generating function. Typically, the line $q = 1$ is a line of finite essential singularities for $x < x_c$. The line $x_c(q)$, where $P(x, q)$ is singular for $q < 1$, is typically a line of logarithmic singularities. For branched polymers in the continuum limit, the logarithmic singularity has been proved recently in [91].

Of special interest is the point $(x_c, 1)$ where these two lines of singularities meet. The behaviour of the singular part of the perimeter and area generating function about $(x_c, 1)$ is expected to take the special form

$$P(x, q) \sim P^{(reg)}(x, q) + (1 - q)^{\theta} F((x_c - x)(1 - q)^{-\phi}), \qquad (x, q) \to (x_c^-, 1^-), \tag{66}$$

where $F(s)$ is a *scaling function* of combined argument $s = (x_c - x)(1 - q)^{-\phi}$, commonly assumed to be regular at the origin, and θ and ϕ are *critical exponents*. The singular behaviour about $q = 1$ at the critical point x_c is then given by $P^{(sing)}(x_c, 1) \sim (1-q)^{\theta} F(0)$. This scaling assumption implies an asymptotic expansion of the scaling function of the form

$$F(s) = \sum_{k=0}^{\infty} \frac{f_k}{s^{(k-\theta)/\phi}}. \tag{67}$$

The leading asymptotic behaviour characterises the singularity of the perimeter generating function via $P(x, 1) \sim f_0(x_c - x)^{-\gamma}$, where $\theta + \phi\gamma = 0$. The first singularity of $F(s)$ on the negative axis determines the singularity along the curve $x_c(q)$. The locus on the axis (say at $s = s_c$) determines the line $x_c(q) \sim x_c - s_c(1 - q)^{\phi}$ near $q = 1$, which meets the line $q = 1$ vertically for $\phi < 1$.

In [76] a similar model was studied analytically using a mapping onto a gauge model. As in other studies, they found the critical behaviour to be governed by a branched polymer fixed point.

More recently, Richard, Guttmann and Jensen [92] have given a very persuasive conjecture as to the exact nature of the scaling function at the bicritical point $(x_c^2, 1)$. In their work, it was natural to work with *rooted* SAP, and in that case the conjectured form of the scaling function was found to be

$$F^{(r)}(s) = \frac{x_c}{\pi\sigma} \frac{d}{ds} \log \mathrm{Ai}\left(\frac{\pi}{x_c} (2E_0)^{\frac{2}{3}} s\right) \tag{68}$$

with exponents $\theta = 1/3$ and $\phi = 2/3$. The conjectured form of the scaling function is then obtained by integration and is

$$F(s) = -\frac{1}{\pi\sigma} \log \mathrm{Ai}\left(\frac{\pi}{x_c}\,(2E_0)^{\frac{2}{3}}\,s\right) \tag{69}$$

with exponents $\theta = 1$ and $\phi = 2/3$. The parameters for the square lattice are $\sigma = 2$ and $x_c = 0.379052277757(5)$. The parameters for the hexagonal lattice are $\sigma = 2$ and $x_c = 1/\sqrt{2+\sqrt{2}}$ (known exactly from the work of Nienhuis [5]) and for the triangular lattice $\sigma = 1$ and $x_c = 0.2409175745(3)$. Further details of this important calculation can be found in [93].

9.7. Macromolecular desorption from a surface

As briefly described above, in this situation we are applying a force perpendicular to an adsorbing surface to which a polymer chain is attached. At low temperature, surface attraction dominates, but at high temperatures entropy dominates, and the polymer is free of the surface. The temperature dependent force needed to extend the polymer is calculated. Let the polymer have N monomers, of which n lie in the surface. (In two dimensions the "surface" is a line). Let $c_N(n, z)$ be the number of such SAW whose endpoint is at perpendicular distance z from the surface. The model may be described by the partition function

$$Z_N(\omega, u) = \sum_{n,z} c_{n,z}\omega^n u^z \tag{70}$$

where $\omega = \mathrm{e}^{-\epsilon/kT}$ and $u = \mathrm{e}^{f/kT}$, where $\epsilon < 0$ is the attractive energy of a monomer with the surface, and f is the force acting on the endpoint monomer, in a direction perpendicular to the surface.

In [96] exactly solvable models based on Dyck paths and Motzkin paths in two dimensions, and a partially directed walk model in three dimensions are given. Orlandini et al. [96] observe re-entrant behaviour in three dimensions, but not in two. Reentrant behaviour is shown in figure 10 below:

"Reentrant behaviour" refers to the fact that the force temperature diagram at first increases with increasing temperature, and then decreases. It thus has a finite maximum at a positive temperature.

Another series study of this problem was given by Marenduzzo et al. [94], who found that the finite length polymer unfolds in multiple steps, as successive bonds break away from the surface. This becomes smoothed out as the length of the SAW tends to infinity. This phenomenon is discussed and illustrated further below. However, their geometry is restricted to a strip of width L, enabling them to use standard transfer matrix methods. As a consequence, they do not enumerate all SAW of a given length. For the two-dimensional lattice they find a reentrant force vs. temperature curve.

In [95] the results of enumeration of interacting SAWs in two dimensions for $N \leq 30$ and in three dimensions for $N \leq 19$ are given. As a result of this study, they report a reentrant force-temperature diagram in three dimensions, but not in two dimensions, exactly as observed in the toy models in [96]. Based on much longer enumerations in two

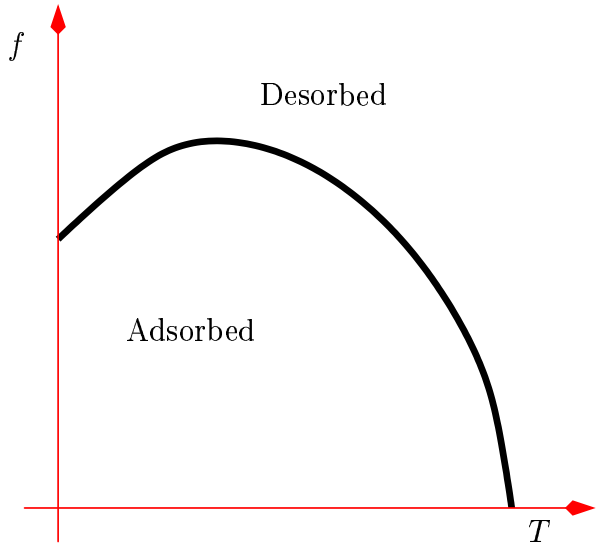

Figure 10. A reentrant force-temperature curve.

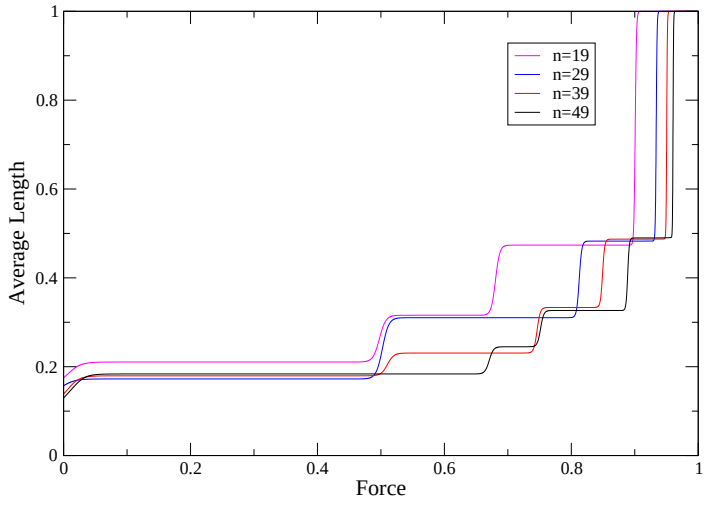

Figure 11. The "stick-release" behaviour of the force-extension curve for walks of various lengths at $T = 0.1$. Lengths increase from the left- to the right-hand curves.

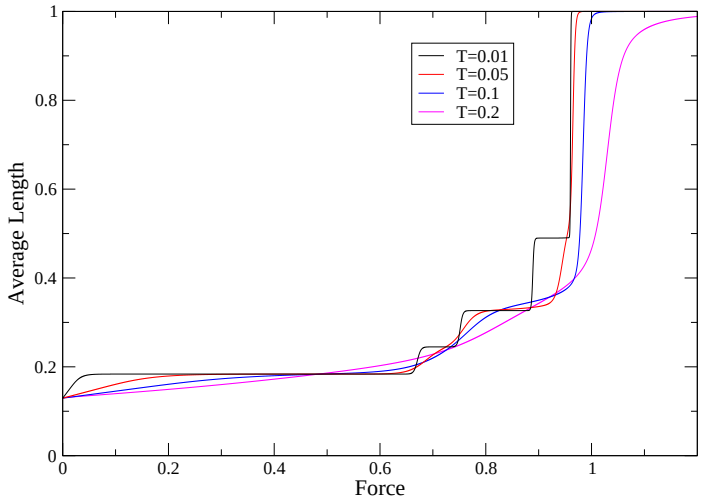

Figure 12. The "stick-release" behaviour of the force-extension curve for 50 step walks at different temperatures. Temperatures increase from the left- to the right-hand curves.

dimensions, to $N = 50$ Jensen and Guttmann [97] obtained clear evidence of a reentrant force-temperature diagram even in two dimensions. The "stick-release" behaviour of SAW pulled from a surface is also clearly shown in that study. In figures 11 and 12 the average length is plotted against applied force. The series of plateaus become smoothed out as the length of the walk increases at fixed temperature, and also as the temperature is raised for SAW of fixed length.

It can be seen from the above selection of series studies that SAW models are capable of shedding light on a wide variety of biological problems. The range of problems that can be addressed in this way seems to be limited only by the imagination of the researchers.

CONCLUSION

In this chapter we have discussed a representative, but far from exhaustive, range of problems which can be usefully modelled by SAW in a random or restricted environment, and which can be successfully studied by series methods. In most cases other approximation techniques are also applicable, and as a general rule one can be much more confident of conclusions drawn from approximate studies from several different methods—provided, of course, that they are self-consistent.

The methods of series generation and analysis is particularly powerful in determining lattice dependent properties. For example, the growth constants of SAW on various lattices is most accurately determined by series methods. Universal properties, such as critical exponents seem to be equally well determined by high-class Monte Carlo work or high class series work. In two dimensions, where finite-lattice methods (FLM) can be applied [50,64], series methods are extremely powerful, and likely to be better than all but the most exhaustive Monte Carlo calculations. Where interactions become very complicated, or of longer range, so that FLM type methods are difficult or impossible

to apply, Monte Carlo methods are often superior. In all situations however, it is useful to seek cross validation from both methods, as well as field theoretical techniques, when applicable.

As can be seen from the above examples, there is a huge range of problems to which SAW can be applied, and the outcome determined by series analysis. In this chapter we have hopefully indicated the ingenuity of many authors in such applications, and it is clear that many more interesting applications will be made in the future.

REFERENCES

1. K. Barat and B. K. Chakrabarti, *Physics Reports* **258** (1995) 377.
2. C. E. Soteros and S. G. Whittington, J. Phys. A: Math. Gen., **37** (2004) R279.
3. B. D. Hughes, *Random walks and random environments*, Clarendon Press, Oxford, (1995).
4. N. Madras and G. Slade, *The Self-Avoiding Walk* (Boston: Birkhäuser) (1993).
5. B. Nienhuis, Phys. Rev. Lett. **49** (1982) 1062.
6. A. J. Guttmann, J. Phys. A: Math. Gen., **17** (1984) 455.
7. H. Kleinert, J. Neu, V. Schulte-Frohlinde, K. G. Chetyrkin and S.A. Larin, Phys. Lett. B **272** (1991), 39, Erratum: ibid **319** (1993) 545.
8. A. B. Harris, Z. Phys. B **49** (1983) 347.
9. Y. Meir and A. B. Harris, Phys. Rev. Letts., **63** (1989) 2819.
10. P. Grassberger, J. Phys A:Math. Gen., **26** (1993) 1023.
11. C. von Ferber, V. Blavats'ka, R. Folk and Yu. Holovatch, *cond-mat/0312065* (2004)
12. K. Kremer, Z. Phys. B, **45** (1981) 149.
13. P. M. Lam, J. Phys. A: Math. Gen., **23** (1990) L831.
14. A. Ordemann, M. Porto, H.E. Roman S. Havlin and A. Bunde, Phys. Rev. E, **61** (2000) 6858
15. T Morita, J. Math. Phys., **5** (1964) 1401.
16. R. D. Martin, Behavior of a random copolymer at the interface between two immiscible solvents, MSc Thesis, University of Toronto, Canada (2000)
17. E. W. James, C. E. Soteros and S. G. Whittington, J. Phys. A: Math. Gen., **36** (2003) 11575.
18. R. D. Martin, M. S. Causo and S. G. Whittington, J. Phys. A: Math. Gen., **33** (2000) 79038.
19. I Golding and Y. Kantor, Phys. Rev. E, **56** (1997) R1318.
20. Y. Kantor and M. Kardar, Europhys. Lett., **28** (1994) 169.
21. P. Monari and L. A. Stella, Phys. Rev. E, **59** (1999) 1887.
22. J. M Hammersley and S. G. Whittington, J. Phys. A: Math. Gen., **18** (1985) 101.
23. M. N. Barber, Phys. Rev. B, **8** (1973) 407.
24. A. J. Guttmann and G. M. Torrie, J. Phys. A: Math. Gen., **17** (1984) 3539.
25. M. Daoud, J. P. Cotton, B. Farnoux, G. Jannick, G. Sarma, H. Benoit, R. Dupplesix, C. Picot and P. G. de Gennes, Macromolecules, **8** (1975) 804.
26. J. L. Cardy, J. Phys. A: Math. Gen., **16** (1983) 3617.
27. J. M. Hammersley, G. M. Torrie and S. G. Whittington, J. Phys. A: Math. Gen., **15** (1982) 539.

28. M. T. Batchelor, D. Bennett-Wood and A. L. Owczarek, Eur. Phys. J., **B 5** (1998) 139.
29. R. Stanley, *Enumerative Combinatorics*, vol. 1, Cambridge Univ. Press, (1997).
30. D. J. Klein, J. Stat. Phys., **23** (1980) 561.
31. M. Daoud and P. G. de Gennes, J. Physique, **38** (1977), 85.
32. C. Soteros and S. G. Whittington, J. Phys. A: Math. Gen., **21** (1988) L857.
33. C. Soteros and S. G. Whittington, J. Phys. A: Math. Gen., **22** (1989) 5259.
34. H. L. Abbott and D. Hanson, Ars Combinatoria, **6** (1978) 163.
35. S. G. Whittington and A. J. Guttmann, J. Phys A:Math. Gen, **23** (1990) 5601.
36. M. Bousquet-Mélou, A. J. Guttmann and I. Jensen, (in preparation) (2005).
37. N. Madras, J. Phys. A: Math. Gen., **28** (1995) 1535.
38. A. J. Guttmann, Phase Transitions and Critical Phenomena vol. 13, (eds. C Domb and J L Lebowitz) (New York: Academic), (1989).
39. F. Gähler P. Kramer H-R. Trebin and K. Urban, Proceedings of the 7th International Conference on Quasicrystals, Mat. Sci. Engin., (2000) 294.
40. P. Repetowicz U Grimm and M. Schreiber, J. Phys. A: Math. Gen., **32** (1999) 4397.
41. P. Repetowicz J. Phys. A: Math. Gen., **35** (2002) 7753.
42. J. M. Luck, Europhys. Lett., **24** (1993) 359.
43. R. Penrose, Bull. Inst. Math. Appl., **10** (1974) 266.
44. P. Kramer and R. Neri, Acta Cryst., **A 40** (1984) 580. Acta Cryst., **A 41** (1984) 619 (Erratum).
45. I. Jensen I and A. J. Guttmann, J. Phys. A: Math. Gen., **31** (1998) 8137.
46. A. N. Rogers, C. Richard and A. J. Guttmann, J. Phys. A: Math. Gen., **36** (2003) 6661.
47. K. Briggs, Int. J. Mod. Phys., **B 7** (1993) 1569.
48. G. Langie and F. Iglói, J. Phys. A: Math. Gen., **25** (1992) L487.
49. C. L. Henley, *Quasicrystals: The State of the Art*, Eds. DiVincenzo D P and Steinhardt P J, Series on Directions in Condensed Matter Physics, vol 16, (Singapore: World Scientific) 2nd edition (1999) 459.
50. I. G. Enting, Nucl. Phys. B (Proc. Suppl), **47** (1996) 180.
51. A. R. Conway, I. G. Enting and A. J. Guttmann, J. Phys. A: Math. Gen, **26** (1993) 1519.
52. A. R. Conway and A. J. Guttmann, Phys. Rev. Letts., **77** (1996) 5284.
53. R. Ammann B. Grünbaum B and G. C. Shephard, Disc. Comp. Geom., **8** (1992) 1.
54. A. Katz, *Beyond Quasicrystals* eds. F. Axel and D. Gratias, (Berlin: Springer) (1995) 141.
55. N. G. de Bruijn, Indagationes Mathematicae (Proc. Kon. Ned. Akad. Wet. Ser. A), **84** (1981) 39 and 53.
56. J. C. Lagarias and P. A. B. Pleasants, Can. Math. Bull., **48** (4) (2002) 634.
57. D. Lenz, (2002) private communication.
58. M. Baake D. Joseph P. Kramer and M. Schlottmann, J. Phys. A: Math. Gen., **23** (1990) L1037.
59. M. Baake and D. Joseph, Phys. Rev. B, **42** (1990) 8091.
60. B. Grünbaum B and G. C. Shephard, *Tilings and Patterns* (New York: Freeman), (1987).

61. R. Sedgewick, *Algorithms in C++*, 2nd ed (Reading: Addison-Wesley) (1992).
62. H. Kesten, J. Math. Phys., **4** (1963) 960.
63. J. M. Hammersley, Phys. Rev., **118** (1960) 656.
64. I. Jensen, J. Phys. A: Math. Gen., **33** (2000) 3533.
65. R. Reitman, B. Nienhuis and J. Oitmaa, J. Phys. A: Math. Gen., **25**, (1992) 6577.
66. E. Swierczak and A. J. Guttmann, J. Phys. A: Math. Gen., **29** (1996) 7485.
67. N. Madras and C. Chris Wu, to appear in Combinatorics, Probability, and Computing, (2005).
68. J. M. Hammersley, Math. Proc. Cambridge Phil. Soc., **57** (1961) 516.
69. R. M. Wartell and A. S. Benight, Phys. Rep., **126** (1985) 67.
70. D. Poland and H. A. Scheraga, J. Chem. Phys., **45** (1966) 1456.
71. D. Poland and H. A. Scheraga, J. Chem. Phys., **45** (1966) 1464.
72. M. E. Fisher, J. Chem. Phys., **45** (1966) 1469.
73. M. E. Fisher, J. Stat. Phys., **34** (1984) 667.
74. S. Leibler, R. R. P. Singh and M. E. Fisher, Phys. Rev. Letts., **59** (1987) 1989.
75. M. E. Fisher, A. J. Guttmann and S. G. Whittington, J. Phys. A: Math. Gen., **24** (1991) 3095.
76. J. A. Banavar, A. Maritan and A. Stella, Phys. Rev. A, **43** (1991) 5752.
77. K. Svoboda and S. M. Block, Ann. Rev. Biophys. Biomol. Struct., **23** (1994) 247.
78. A. Ashkin, Proc. Natl. Acad. Sci. USA, **94** (1997) 4853.
79. M. S. Causo, B. Coluzzi and P. Grassberger, Phys. Rev. E, **62** (2000) 3958.
80. E. Carlon, E. Orlandini and A. L. Stella, Phys. Rev. Lett., **88** (2002) 198101.
81. M. Baiesi, E. Carlon and A. L. Stella, Phys. Rev. E, **66** (2002) 21804.
82. M. Baiesi, E. Carlon, Y. Kafri, D. Mukamel, E. Orlandini and A. L. Stella, Phys. Rev. E, **67** (2002) 21911.
83. Y. Kafri, D. Mukamel and L. Peliti, Phys. Rev. Lett., **85** (2000) 4988.
84. Y. Kafri, D. Mukamel and L. Peliti, Eur. Phys. J. B, **27** (2001) 135.
85. Y. Kafri, D. Mukamel and L. Peliti, Physica A, **306** (2002) 39.
86. A. Hanke and R. Metzler, Phys. Rev. Letts., **90** (2003) 159801.
87. M. Baiesi, E. Carlon, E. Orlandini and A. L. Stella, Eur. Phys. J. B, **29** (2002) 129.
88. A. Hanke and R. Metzler, Biophysical Journal, **85** (2003) 167.
89. C. Richard and A. J. Guttmann, J. Stat. Phys., **115** (3/4) (2004) 925.
90. E. J. Janse van Rensburg, *The Statistical Mechanics of Interacting walks, Polygons, Animals and Vesicles*, Oxford University Press, New York (2000).
91. D. C. Brydges and J. Z. Imbrie, Ann. Math., **158** (2003) 1019.
92. C. Richard A. J. Guttmann and I. Jensen, J. Phys. A: Math. Gen., **34** (2001) L495.
93. C. Richard, J. Stat. Phys., **108** Nos. 3/4, (2002) 459.
94. D. Marenduzzo, A. Maritan, A. Rosa and F. Seno, Phys. Rev. Letts., **90** (2003) 088301.
95. P. K. Mishra, S. Kumar and Y. Singh, Europhys. Letts., (to appear) (2004).
96. E. Orlandini, M. Tesi and S. G. Whittington, J. Phys. A: Math. Gen., **34** (2004) 1535.
97. I. Jensen and A. J. Guttmann, Stretching of a polymer adsorbed on a surface, (in preparation).